

Dear Reviewer,

The authors sincerely appreciate your valuable comments and suggestions to help improve the manuscript. We have revised the manuscript titled “Estimating the Snow Density using Collocated Parsivel and MRR Measurements: A Preliminary Study from ICE-POP 2017/2018 ”. that was submitted to ACP (Atmospheric Chemistry and Physics) on 3 January, 2024. Based on your suggestions, we have put substantial effort into additional analysis. The manuscript has been thoughtfully revised regarding the comments from all reviewers.

One of the major concerns of the proposed density retrieval algorithm using collocated MRR and Parsivel is lacking the uncertainty analysis. As per the reviewer’s suggestion, we have performed substantial investigations of the retrieval uncertainty. The impacts of the measurement uncertainty of the Parsivel and the MRR on the bulk density retrieval are analyzed quantitatively. The measurement issue of Parsivel is also investigated to understand its impact on bulk density retrieval. The results are summarized in the revised manuscript as a Discussion section.

The MRR data quality issue has been examined per the reviewer’s suggestion. The post-processed data have replaced the entire MRR raw data by applying the algorithm from Maahn and Kollias (2012). All the bulk density, bulk water fraction, and reflectivity-weighted velocity retrievals have been recalculated. The figures have been revised as well.

The original purpose of utilizing reflectivity-weighted velocity to filter adequate retrieval is no longer needed and has been removed in the revised manuscript. The quality of the retrieval results has been greatly improved by applying the post-processed MRR data per the reviewer’s suggestion. The low SNR MRR measurement has been removed. The comparison of reflectivity-weighted velocity is mainly used to identify the inadequate retrieval due to the attenuation effect on MRR reflectivity.

The performance of the retrieved bulk density has been validated by the snowfall rate (SR) from collocated Pluvio measurements and reflectivity-weighted fall velocity (V_z) from MRR. In addition to SR and V_z , the performance of the retrieved bulk density has been compared with the precipitation imaging package (PIP), a video disdrometer (Newman et al., 2009; Pettersen et al., 2020). The PIP was also deployed at the MHS site during ICE-POP 2018 (Tokay et al., 2023). The comparison of retrieved bulk density between the proposed algorithm in this study and PIP has shown good agreement with each other. The high consistency further confirms the performance of the retrieved bulk density. Since there is no direct bulk water fraction measurement for validation, the authors consider the validation of bulk density retrieval to PIP and Pluvio as “indirect” evidence to support the bulk water fraction retrieval.

The SR and Vz validation analysis shows that the algorithm can adequately retrieve the bulk density and bulk water fraction. The consistency of the retrieved bulk density to collocated PIP confirms the performance of the proposed algorithm in this study. The advantage of the proposed algorithm is that it utilizes collocated Parsivel and MRR, which are commercially available, commonly used, and robust instruments. The Parsivel and MRR can operate unattended and need little maintenance. Further application of the proposed algorithm helps derive long-term observation data on snow properties. The authors believe the proposed algorithm can provide an alternative choice if sophisticated instruments (e.g., 2DVD, PIP, SVI, MASC) are unavailable.

The manuscript has also been revised carefully following the reviewer's suggestions on English wording. The authors would like to express our sincere appreciation for the comments. The added or modified sentences in the revised manual are in red for your convenience.

The point-to-point replies to every comment have been prepared in the following. For your convenience, the reply is arranged as follows,

Reviewer's comments

Response

Revisions in the manuscript

We would appreciate any feedback on the revisions.

General comments

Do the authors see a possibility that the retrieved high values of bulk density and liquid fraction during periods of low reflectivity and precipitation rate could be, at least partly, an artifact from applying the method on observations of very weak precipitation? The retrieval seems somewhat unstable in these conditions which is not surprising considering factors such as low signal to noise ratio due to weak signal. Yet, the authors draw considerable attention to the retrievals of these periods of very weak precipitation. It is worth considering which disciplines would benefit from the microphysical retrievals of weak mixed phase precipitation (<0.5mm/h)? I would suggest either introducing a threshold for minimum reflectivity or precipitation rate where the method is applied, or otherwise critically reviewing the method's performance in weak precipitation, where the precipitation rate falls below the sensitivity of the Pluvios.

Reply: The retrieved bulk density and bulk water fraction as a function of density are shown in Figure R1. Most retrieved bulk density is obtained from MRR reflectivity from 10 to 30 dBZ. Some retrieval results with high bulk density and low MRR reflectivity can be found, but not frequent.

The quality of the retrieval results has been greatly improved by applying the post-processed MRR data as per the reviewer's suggestion. The low SNR MRR measurement has been removed. The authors intend to preserve as much data as possible by only eliminating the data with an attenuation effect on MRR reflectivity. The attenuated MRR reflectivity underestimates the retrieved bulk density and bulk water fraction.

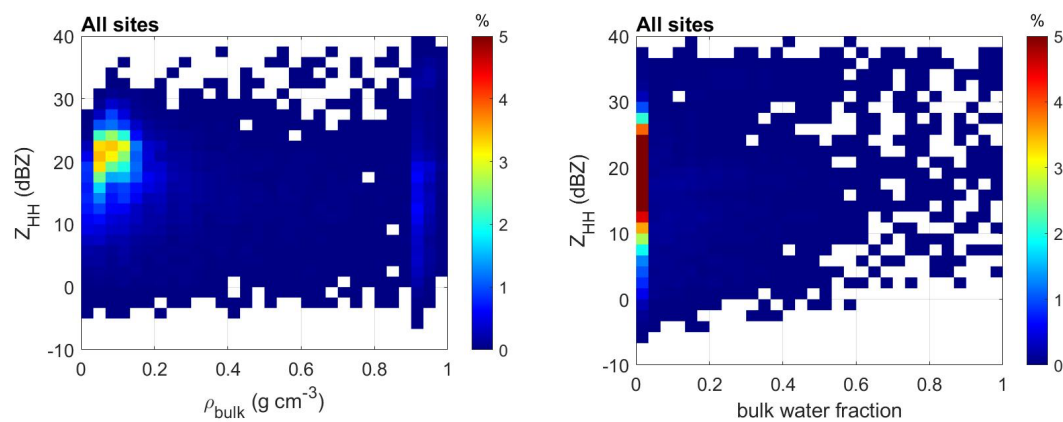


Figure R1: (a) The retrieved bulk density as a function of MRR reflectivity. (b) Same as (a), but for bulk water fraction.

I don't feel that the retrieval of v_w is adequately demonstrated in the case studies since there seem to be no time periods where there would be both a) agreement between derived and measured terminal velocity and b) notable precipitation intensity at the same time. It raises the concern how the method would perform in mixed phase situations with larger particles or higher precipitation rates. In my mind, the best way to address this would be to replace one of the case studies with another one that has significant intensity of wet snow, or discuss the possible limitations of the method's application.

Reply: The bulk water fraction is derived along with the maximum possible bulk density using the proposed method in this study. If a different assumption is made when selecting possible bulk density, the retrieved bulk water fraction will be different. Therefore, the performance of the retrieved bulk water fraction is linked with bulk density retrieval. Since there is no direct measurement of bulk water fraction, we compare the retrieved bulk density from the proposed method and PIP. The consistency between retrieved bulk density from the two algorithms strengthens the reliability of the retrieved bulk water, which should be reasonable.

As shown in Fig. R2(a), the retrieved bulk density values from the proposed algorithm and PIP gradually decrease from nearly 1.0 to 0.1 (g cm^{-3}) between 03 and 06 UTC. Both algorithms capture the transition from the mixing phase to dry snow. Please see Figure R2. The manuscript has been revised to include a bulk water fraction retrieval discussion.

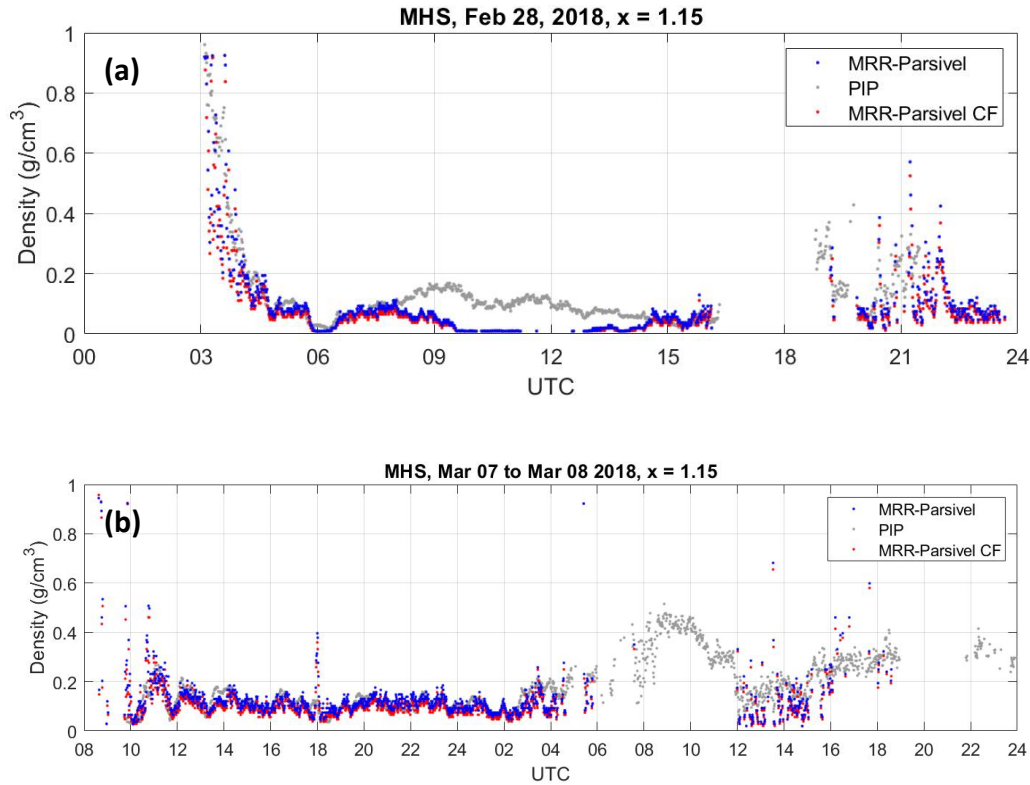


Figure R2: (a) The retrieved bulk density from collocated MRR and Parsivel. The blue dots are retrieved from CF-adjusted PSD. The red dots are from the original PSD. The gray dots are the retrieval from PIP. The case is 28 February 2018. (b) Same as (a), but for case 7 March 2018.

Please see the following and Line 398-417 of the revised manuscript.

The precipitation imaging package (PIP), a video disdrometer, provides the PSD, fall speed, density, and snowfall rate of hydrometers (Newman et al., 2009; Pettersen et al., 2020) was also deployed at the MHS site during ICE-POP 2018. Tokay et al. (2023) have utilized PIP to investigate the PSD parameters, including mass-weighted diameter and normalized intercept. The bulk density is estimated by Tokay et al. (2023) with various assumptions. The PIP retrieved density was generated from the assumption that $D_{\text{max}} = 1.15 D_{\text{eq}}$, and the mass derivation included was based on Bohm (1989). As shown in Fig. 15, the retrieved bulk density from the proposed algorithm in this study and PIP have high consistency. Both retrieved bulk densities are highly correlated to each other, except for the period of 08 to 15UTC on 28

February due to the attenuation effect of the accumulated snow on the MRR antenna (Fig. 5e).

The bulk water fraction is derived along with the maximum possible bulk density using the proposed method in this study. The retrieved bulk water fraction will differ if a different assumption is made when selecting possible bulk density. Therefore, the performance of the retrieved bulk water fraction is linked with bulk density retrieval. Since there are no direct measurements of bulk water fraction, the consistency between retrieved bulk density from two algorithms “indirectly” confirms that the retrieved bulk water should be reasonable. As shown in Fig. 15a, the retrieved bulk density values from the proposed algorithm and PIP gradually decrease from nearly 1.0 to 0.1 (g cm^{-3}) between 03 and 06 UTC. Both algorithms capture the fast transition from the mixing-phase to dry snow.

Despite the various possible factors that can degrade the performance of bulk density retrieval from collocated MRR and Parsivel, the uncertainty study has shown that the retrieval performance has an acceptable low impact by the Parsivel and MRR observational error. The agreement between this study and PIP retrieval further confirms that the proposed algorithm can robustly retrieve the bulk density and water fraction from collocated MRR and Parsivel.

The proposed retrieval technique has been applied to all available events (listed in Table 1), and the results are summarized in Figure 14. The coastal sites (BKC and GWU) were associated with higher retrieved bulk water fraction. The environment parameters, including temperature ($^{\circ}\text{C}$) and vapor pressure (hPa), show that the coastal sites have higher temperatures and more water vapor. It is postulated that the high bulk water fraction retrievals with higher temperatures and more water vapor are likely wet snow events. Please see the following and Line 339-357 of the revised manuscript.

To further understand the microphysical characteristics of winter precipitation, each site's retrieved bulk density and bulk water fractions are divided into warm-low (nine cases) and cold-low (five cases) events according to the synoptic condition (Gehring et al. 2020; Kim et al. 2021). As shown in Fig. 14a, the median values of bulk density of warm-low events from the mountain site (YPO) to the coastal site (GWU) are about 0.10 to 0.29 g cm^{-3} . The GWU site has the highest bulk density. On the other hand, the median values of bulk density of cold-low events from YPO to GWU are about 0.07 to 0.05 g cm^{-3} (Fig. 14b). The overall bulk density values are lower in cold-low events than in warm-low events.

In Fig. 14c and d, more than 90% of bulk water fractions are less than 0.03 for warm- and cold-low events. The YPO site has the lowest bulk water fraction, especially the cold-low events that remain lower than 0.22. The mean value of the top 5% of the bulk water fraction of each site is obtained for further investigation. The values of bulk water fraction gradually increase from the mountain site (YPO) to the coastal site (GWU) for both warm- and cold-low events. The mean values of the top 5% bulk water fraction of YPO, MHS, and CPO sites for warm-low events are 0.0015, and the BKC and GWU are about 0.32 to 0.45. The cold-low

events are 0.0013 to 0.19 for each site.

The temperature ($^{\circ}\text{C}$) and water vapor pressure (hPa) measurements from nearby mountain and coastal AWS sites are collected and summarized in Fig. 14e. Warm-low events have warmer and moister conditions than cold-low events. The coastal area's warm- and cold-low events have similar mean temperature values. On the other hand, the water vapor pressure increases significantly from cold-low to warm-low events in the coastal region. The mountain area has similar features, but higher temperature increments and fewer increments of water vapor pressure. These results indicate that the winter precipitation systems of coastal sites with warmer and moister environments have higher bulk density and bulk water fraction than mountain sites.

The limitations of the proposed bulk density retrieval method have been discussed in the revised manuscript. Please see the following and “Discussion” section of the revised manuscript.

5 Discussion

The proposed retrieval algorithm has shown that it can estimate the bulk density and bulk water fraction with reasonable performance. The underestimation of retrievals caused by the attenuation effect of MRR reflectivity can be well identified by reflectivity-weighted velocity. In addition to the attenuation effect, the uncertainties of the retrieval algorithm can be attributed to observational data quality and the algorithm's basic assumption. In the following discussion, Parsivel's PSD measurement uncertainty will be investigated. In addition, the impact of bulk density and water fraction retrieval from spherical particle assumption and the uncertainty of MRR reflectivity measurement will be discussed.

5.1 The measurement uncertainty of Parsivel fall velocity and its impact on the bulk density and water fraction retrieval

As indicated by the study by Battaglia et al. (2010) and Wood et al. (2013), Parsivel's fall velocity measurement may not be accurate for a snowflake particle. This issue is due to the internally assumed relationship between horizontal and vertical snow particle dimensions. Yuter et al. (2006), Aikins et al. (2016), and Kim et al. (2021) indicate the splashing and border effects of the diameter of < 1 mm in Parsivel fall velocity measurements. The fall velocity issue explains why the consistently high fall velocity of diameter less than 1 mm in the MHS site can be noticed by the fall velocity-diameter relation in Figs. 6 and 12; even the retrieved bulk density and water fraction were low and should be associated with low fall velocity. Yuter et al. (2006) and Aikins et al. (2016) suggest a quality control procedure that discards particles with a diameter of < 1 mm to avoid splashing and border effects.

As Battaglia et al. (2010) indicated, the Parsivel overestimates the snowfall velocity and underestimates the PSD. A correction factor (CF) derived from comparing the collocated 2DVD in the MHS site is suggested by Dr. Gyuwon Lee (personal communication). The particle size-dependent CF adjusts the fall velocity measurement from Parsivel and thus modifies the PSD. The CF reduces the fall velocity to a factor of two as the particle size is around 10 μm . The modified PSD has a higher concentration after applying CF adjustment. The bulk density and water fraction retrieval uncertainty due to PSD measurement issues are investigated using the PSD and CF-adjusted PSD. As shown in Fig. 15, the bulk density retrieval decreases slightly after applying CF-adjusted PSD in the 28 February and the 7 March 2018 events. The bias of retrieved bulk density is about $-0.0153 \text{ (g cm}^{-3}\text{)}$, and the standard deviation is about $0.095 \text{ (g cm}^{-3}\text{)}$. The bias and the standard deviation for bulk water fraction - 1.8×10^{-4} and 2.6×10^{-3} .

The results indicate that with the measurement uncertainty of PSD from Parsivel, the bulk density and water fraction retrieval are fairly low. It is postulated that fall velocity measurement uncertainty slightly impacts the PSD calculation; thus, the bulk density and water fraction retrieval uncertainty is sufficiently low.

5.2 The measurement uncertainty of MRR reflectivity and its impact on the bulk density and water fraction retrieval

The simulation of MRR reflectivity can be sensitive to the particle shape assumption. A sensitivity investigation assuming the particle axis ratio of 0.5 shows that about 1.5 dBZ variation of MRR reflectivity can be induced. Another possible source of retrieval uncertainty is the measurement of MRR reflectivity. As discussed in the MRR bias calculation from pure rain events, the standard deviation between MRR reflectivity and Parsivel calculated reflectivity is about 1.1 to 1.3 dBZ for each site. A random error of MRR reflectivity with a standard deviation of 1.2 dB is introduced into the retrieval algorithm to imitate the particle assumption and MRR measurement uncertainty. In Figure 16(a), the algorithm overestimates the bulk density ($\Delta\rho^{bulk} > 0$) as the MRR reflectivity's positive error ($\Delta Z_{HH} > 0$) increases. On the other hand, the negative bias of MRR reflectivity ($\Delta Z_{HH} < 0$) led to an underestimation of the bulk density retrieval ($\Delta\rho^{bulk} < 0$). The overall standard deviation of bulk density retrieval uncertainty is about $0.025 \text{ (g cm}^{-3}\text{)}$ for a given MRR reflectivity uncertainty of 1.2 dB. The bulk water fraction retrieval has the same feature shown in Fig. 16(b). Given an MRR reflectivity uncertainty of 1.2 dB, the bulk water fraction retrieval uncertainty is about 0.041.

5.3 The bulk density comparison with collocated PIP

The precipitation imaging package (PIP), a video disdrometer, provides the PSD, fall speed,

density, and snowfall rate of hydrometers (Newman et al., 2009; Pettersen et al., 2020) was also deployed at the MHS site during ICE-POP 2018. Tokay et al. (2023) have utilized PIP to investigate the PSD parameters, including mass-weighted diameter and normalized intercept. The bulk density is estimated by Tokay et al. (2023) with various assumptions. The PIP retrieved density was generated from the assumption that $D_{\max} = 1.15 D_{\text{eq}}$, and the mass derivation included was based on Bohm (1989). As shown in Fig. 15, the retrieved bulk density from the proposed algorithm in this study and PIP have high consistency. Both retrieved bulk densities are highly correlated to each other, except for the period of 08 to 15UTC on 28 February due to the attenuation effect of the accumulated snow on the MRR antenna (Fig. 5e).

The bulk water fraction is derived along with the maximum possible bulk density using the proposed method in this study. The retrieved bulk water fraction will differ if a different assumption is made when selecting possible bulk density. Therefore, the performance of the retrieved bulk water fraction is linked with bulk density retrieval. Since there are no direct measurements of bulk water fraction, the consistency between retrieved bulk density from two algorithms “indirectly” confirms that the retrieved bulk water should be reasonable. As shown in Fig. 15a, the retrieved bulk density values from the proposed algorithm and PIP gradually decrease from nearly 1.0 to 0.1 (g cm^{-3}) between 03 and 06 UTC. Both algorithms capture the fast transition from the mixing-phase to dry snow.

Despite the various possible factors that can degrade the performance of bulk density retrieval from collocated MRR and Parsivel, the uncertainty study has shown that the retrieval performance has an acceptable low impact by the Parsivel and MRR observational error. The agreement between this study and PIP retrieval further confirms that the proposed algorithm can robustly retrieve the bulk density and water fraction from collocated MRR and Parsivel.

In the presented case studies, it seems like non-zero v_w values only occur when bulk density is nearly saturated at over 0.9 g/cm. I'm concerned whether this is physically reasonable especially given the assumption of spherical particles. This raises the question whether, effectively, the liquid fraction would act as a kind of an overflow buffer in the calculations when density alone cannot explain the reflectivity values. This could rise from the assumption of maximum ice volume fraction (v_i). Or could it be explained with the drizzle-like nature of the precipitation during the v_w signals? This concern could be dispelled with a counter example.

Reply: The assumption of the particle shape has been discussed in the revised manuscript. Please see Lines 386-397 in the revised manuscript or the following.

The simulation of MRR reflectivity can be sensitive to the particle shape assumption. A sensitivity investigation assuming the particle axis ratio of 0.5 shows that about 1.5 dBZ variation of MRR reflectivity can be induced. Another possible source of retrieval uncertainty is the measurement of MRR reflectivity. As discussed in the MRR bias calculation from pure

rain events, the standard deviation between MRR reflectivity and Parsivel calculated reflectivity is about 1.1 to 1.3 dBZ for each site. A random error of MRR reflectivity with a standard deviation of 1.2 dB is introduced into the retrieval algorithm to imitate the particle assumption and MRR measurement uncertainty. In Figure 16(a), the algorithm overestimates the bulk density ($\Delta\rho^{bulk} > 0$) as the MRR reflectivity's positive error ($\Delta Z_{HH} > 0$) increases. On the other hand, the negative bias of MRR reflectivity ($\Delta Z_{HH} < 0$) led to an underestimation of the bulk density retrieval ($\Delta\rho^{bulk} < 0$). The overall standard deviation of bulk density retrieval uncertainty is about $0.025 \text{ (g cm}^{-3}\text{)}$ for a given MRR reflectivity uncertainty of 1.2 dB. The bulk water fraction retrieval has the same feature shown in Fig. 16(b). Given an MRR reflectivity uncertainty of 1.2 dB, the bulk water fraction retrieval uncertainty is about 0.041.

As the reply to the previous comment, the bulk water fraction is derived along with the maximum possible bulk density in the proposed method in this study. The performance of the retrieved bulk water fraction is linked with bulk density retrieval. Since there is no direct measurement of bulk water fraction, we compare the retrieved bulk density from the proposed method and PIP. The consistency between retrieved bulk density from the two algorithms strengthens the reliability of the retrieved bulk water, which should be reasonable. Please see Figure R2. The discussion of bulk water retrieval can be found in Lines 398-417 of the revised manuscript. Or see the following.

The precipitation imaging package (PIP), a video disdrometer, provides the PSD, fall speed, density, and snowfall rate of hydrometers (Newman et al., 2009; Pettersen et al., 2020) was also deployed at the MHS site during ICE-POP 2018. Tokay et al. (2023) have utilized PIP to investigate the PSD parameters, including mass-weighted diameter and normalized intercept. The bulk density is estimated by Tokay et al. (2023) with various assumptions. The PIP retrieved density was generated from the assumption that $D_{max} = 1.15 D_{eq}$, and the mass derivation included was based on Bohm (1989). As shown in Fig. 15, the retrieved bulk density from the proposed algorithm in this study and PIP have high consistency. Both retrieved bulk densities are highly correlated to each other, except for the period of 08 to 15UTC on 28 February due to the attenuation effect of the accumulated snow on the MRR antenna (Fig. 5e).

The bulk water fraction is derived along with the maximum possible bulk density using the proposed method in this study. The retrieved bulk water fraction will differ if a different assumption is made when selecting possible bulk density. Therefore, the performance of the retrieved bulk water fraction is linked with bulk density retrieval. Since there are no direct measurements of bulk water fraction, the consistency between retrieved bulk density from two algorithms “indirectly” confirms that the retrieved bulk water should be reasonable. As shown in Fig. 15a, the retrieved bulk density values from the proposed algorithm and PIP gradually decrease from nearly 1.0 to 0.1 (g cm^{-3}) between 03 and 06 UTC. Both algorithms capture the

fast transition from the mixing-phase to dry snow.

Despite the various possible factors that can degrade the performance of bulk density retrieval from collocated MRR and Parsivel, the uncertainty study has shown that the retrieval performance has an acceptable low impact by the Parsivel and MRR observational error. The agreement between this study and PIP retrieval further confirms that the proposed algorithm can robustly retrieve the bulk density and water fraction from collocated MRR and Parsivel.

The manuscript lacks discussion on the implications of assuming spherical particles. This might be significant consideration given the wide range of different particle habits and their shapes and preferred falling alignments.

Reply: The discussion of the assuming spherical particles has been included in the revised manuscript. Please see Lines 386-397. Or the reply of the previous question.

The particle shape assumption for falling velocity and reflectivity calculation has been discussed. Please see Lines 218-221 in the revised manuscript. Or see the following.

The various shapes aerodynamically complicate the falling behaviors of ice-phase and mixed-phase particles (Mitchell and Heymsfield 2005; Heymsfield and Westbrook 2010). Moreover, various measurement issues of MRR and Parsivel also induce some inconsistency. Nevertheless, the overall consistency of the V_Z^{MRR} and V_Z^{Pbulk} suggests that the retrieved bulk density is an adequately reasonable value.

Since the manuscript considers the liquid fraction, it would be worth showing or at least mentioning if melting layer signals were detected in the MRR observations.

Reply: Most cases in this study have surface temperatures near zero or lower than zero degrees. As shown in Figures 5 and 7-11, there is no pronounced bright-band signature from MRR radar data.

The viewpoint in the manuscript is more technical and focuses less on microphysics. As such, the topic is suitable for ACP but might be even better suited for AMT. This is a possible consideration for resubmission after revisions.

Reply: The manuscript contains the retrieval technique description and the retrieval result analysis. The retrieval technique is demonstrated by substantial bulk density analysis and water fraction evolution. The features of these bulk properties of warm-low and cold-low events are also investigated.

Specific comments

The title refers to snow density, but retrievals are attempted for snow, mixed phase precipitation and light drizzle. If liquid fraction plays an important role in the revised manuscript, it would be good to be reflected in the title.

Reply: The majority of the particles in this study are snow. The algorithm estimates bulk water fraction value, and the mixing phase of snow can be subsequently differentiated from dry snow. As the bulk water fraction equals one, thus the particle is considered a drizzle or raindrop. Hence, the main objective is to estimate the snow bulk density, including dry and wet snow.

The title indicates this is a preliminary study. Are the authors working on a more comprehensive analysis? Worth mentioning in the discussion.

Reply: The proposed method has been introduced and applied to ICE-POP 2018 data. The analysis also shows that the algorithm can adequately retrieve the bulk density and bulk water fraction. The advantage of the proposed algorithm is that it utilizes collocated Parsivel and MRR, which are commonly used and robust instruments. The Parsivel and MRR can operate unattended and need little maintenance. Further application of the proposed algorithm helps derive long-term observation data on snow properties. The discussion has been added to the revised manuscript. **Please see Lines 441-447 in the revised manuscript. Or see the following.**

The SR and Vz validation analysis shows that the algorithm can adequately retrieve the bulk density and bulk water fraction. The consistency of the retrieved bulk density to collocated PIP confirms the performance of the proposed algorithm in this study. The advantage of the proposed algorithm is that it utilizes collocated Parsivel and MRR, which are commercially available, commonly used, and robust instruments. The Parsivel and MRR can operate unattended and need little maintenance. The proposed algorithm provides an alternative choice if a sophisticated instrument (e.g., 2DVD, PIP, SVI, MASC, etc.) is unavailable. Further application of the proposed algorithm helps derive long-term observation data on snow properties.

L42: This sentence seems to suggest that riming and melting are the only processes affecting snow density. While these are important, one should not forget that, e.g., the primary particle habit and aggregation have great impact, too.

Reply: The aggregation process has been added to the revised manuscript. Please see Lines 31-32 in the revised manuscript. Or see the following.

The snow density caused by various degrees of riming, melting, and aggregation processes is essential to derive the Ze-SR relation (Huang et al. 2014).

L59: As one of the selling points of the new density retrieval method is the use of robust instruments that require little maintenance, perhaps it would be good to mention studies that use, e.g., PIP or Parsivel for density retrievals. Such studies could be found, for example, by doing citation analysis on Brandes et al. (2007) and Huang et al. (2010), as referred to in the manuscript.

Reply: Per the reviewer's suggestion, the PIP (precipitation imaging package, Newman et al., 2009; Pettersen et al., 2020) was also deployed at the MHS site during ICE-POP 2018. Tokay et al. (2023) have utilized PIP to investigate the PSD parameters, including mass-weighted diameter and normalized intercept. The bulk density is estimated by Tokay et al. (2023) with various assumptions. The PIP retrieved density was generated from the assumption that $D_{\max} = 1.15 D_{\text{eq}}$, and the mass derivation included was based on Bohm (1989). The time series of retrieved bulk density from the proposed algorithm and PIP are shown in Fig. R2. The consistency between retrieved bulk density from the two algorithms confirms that the retrieved bulk water should be reasonable. Please see Lines 398-413 in the revised manuscript. Or see the following.

5.3 The bulk density comparison with collocated PIP

The precipitation imaging package (PIP), a video disdrometer, provides the PSD, fall speed, density, and snowfall rate of hydrometers (Newman et al., 2009; Pettersen et al., 2020) was also deployed at the MHS site during ICE-POP 2018. Tokay et al. (2023) have utilized PIP to investigate the PSD parameters, including mass-weighted diameter and normalized intercept. The bulk density is estimated by Tokay et al. (2023) with various assumptions. The PIP retrieved density was generated from the assumption that $D_{\max} = 1.15 D_{\text{eq}}$, and the mass derivation included was based on Bohm (1989). As shown in Fig. 15, the retrieved bulk density from the proposed algorithm in this study and PIP have high consistency. Both retrieved bulk densities are highly correlated to each other, except for the period of 08 to 15UTC on 28 February due to the attenuation effect of the accumulated snow on the MRR antenna (Fig. 5e).

The bulk water fraction is derived along with the maximum possible bulk density using the proposed method in this study. The retrieved bulk water fraction will differ if a different assumption is made when selecting possible bulk density. Therefore, the performance of the retrieved bulk water fraction is linked with bulk density retrieval. Since there are no direct measurements of bulk water fraction, the consistency between retrieved bulk density from two

algorithms “indirectly” confirms that the retrieved bulk water should be reasonable. As shown in Fig. 15a, the retrieved bulk density values from the proposed algorithm and PIP gradually decrease from nearly 1.0 to 0.1 (g cm⁻³) between 03 and 06 UTC. Both algorithms capture the fast transition from the mixing-phase to dry snow.

In addition, the MASC (multi-angle snowflake camera) is also introduced in the revised manuscript. Please see Lines 59-62 in the revised manuscript. Or see the following.

Other sophisticated instrumentations are developed to investigate the microphysical characteristics of snow particles. The precipitation imaging package (PIP), a video disdrometer, provides the PSD, fall speed, density, and snowfall rate of hydrometers (Newman et al., 2009; Pettersen et al., 2020). The Multi-Angle Snowflake Camera (MASC) captures high-resolution photographs of hydrometeors from three angles while simultaneously measuring their fall speed (Garrett et al. 2012).

Section 2: Details about the ambient temperature measurements are missing, in particular, the types of the instruments or sensors used. The temperature measurements, while not part of the main retrieval methods presented, should be of great interest for the reader as an indication for melting and other microphysical processes.

Reply: The temperature measurements were derived from collocated AWS (Vaisala WXT520). The comparison between the temperature measurements from AWS and PARSIVEL has shown that WXT520 has better performance. The Parsivel data had a significant bias in the Parsivel temperature data. The information on the temperature sensor has been added to the revised manuscript. Please see Fig. 5, 7-11 in the revised manuscript. Or see the following.

The temperature (°C, red line) from nearby AWS (Vaisala WXT520) and Z_{HH} from the third layer of MRR.

Section 2: I would like to see basic information about the Pluvios used such as make, orifice size and shielding.

Reply: The Pluvios are OTT Pluvio² - Weighing Rain Gauge. All of the Pluvios were equipped with double windshields. The Pluvio at the MHS was within the DFIR (double fence intercomparison reference) in addition to the double shield. All the sites investigated in this study have no taller trees or buildings near the MRR antenna and Parsivel. The environmental conditions of all sites are introduced in the revised manuscript. Please see Lines 92-103 in the revised manuscript. Or see the following.

The data of MRR, Parsivel, and Pluvio (OTT Pluvio² - Weighing Rain Gauge) were collected during the ICE-POP 2018 (2017/2018 winter) and the pre-ICE-POP campaign (2016/2017 winter). The instruments were located in nineteen sites across the Gangwon region on the east coast of Korea (see Kim et al. 2021 for detailed information of each site). Five sites with collocated MRR and Parsivel were available for this study. These sites aligned across the Taebaek Mountains from mountain to coast are YPO (YongPyong Observatory, 772 m MSL), MHS (MayHills Supersite, 789 m MSL), CPO (Cloud Physics Observatory, 855 m MSL), BKC (BoKwang 1-ri Community Center, 175 m MSL), and GWU (Gangneung-Wonju National University, 36 m MSL), respectively. The YPO, MHS, and CPO sites are in the mountainous region, while GWU and BKC sites are in the coastal area (Kim et al. 2021). All of the Pluvios were equipped with double windshields. The Pluvio at the MHS was within the DFIR (double fence intercomparison reference) in addition to the double shield. All the sites investigated in this study have no taller trees or buildings near the MRR antenna and Parsivel. Each site's detailed layout and information can be found in Kim et al. (2021).

L130: What is meant by a canting angle when referring to spherical particles?

Reply: The discussion of non-spherical particles has been introduced in the revised manuscript. Non-spherical and spherical particle measurements are different when MRR looks upward. However, the orientation of the non-spherical particle is assumed to be isotropic and homogeneous. A sensitivity investigation assuming the particle axis ratio of 0.5 has been conducted. The results show that about 1.5 dBZ variation of simulated reflectivity can be induced due to the assumption of particle size.

A random error of MRR reflectivity with a standard deviation of 1.2 dB is introduced into the retrieval algorithm to imitate the particle assumption and MRR measurement uncertainty. The overall standard deviation of bulk density retrieval uncertainty is about 0.025 (g cm⁻³) for a given MRR reflectivity uncertainty of 1.2 dB. The bulk water fraction retrieval has the same feature, and the uncertainty is about 0.041. Please see the Discussion section in the revised manuscript. Or pages 6-8 of this reply.

L133: Why was this temperature range chosen for the simulations? Is it physically reasonable to simulate mixed-phase precipitation in -10 degrees Celsius, for example?

Reply: The temperature is set to 0°C in the T-matrix simulation. The sensitivity test of temperature is shown in Fig. 1. The results indicate that the reflectivity simulation is insensitive to particle temperature. Please see Lines 150-155 in the revised manuscript. Or see the following.

An example of simulated Z_{HH} from Parsivel observed snow PSD via T-matrix simulation with different combination of v_i/v_w and temperature is shown in Fig. 1. The results indicate that the simulated Z_{HH} values remain nearly identical when varying the temperature from -10 to 0 °C. On the other hand, the simulated Z_{HH} varies significantly when altering the composition of v_i/v_w . The lowest (highest) value of Z_{HH} was from the combination of v_i/v_w of 1.0/0.0 (0.0/1.0), which was pure ice (rain) with a density of 0.92 (1.0) g cm⁻³. The particle temperature was consequently assumed to have a constant value of 0 °C in the following Z_{HH} T-matrix simulation.

L147: I failed to find references to liquid water fraction from Huang et al. (2010). They seem to just assume particles to consist of ice and air. Either I missed it, or this reference could be more accurate.

Reply: Huang et al. (2010) assumed that a mixture of snow contains only ice and air. Please see page 642 of Huang et al. (2010), “To calculate the backscattering properties of the particles measured by the 2DVD, we consider snow to be a mixture of ice and air.”

The manuscript has been revised to improve the clarity. Please see Lines 167-168 in the revised manuscript. Or see the following.

This assumption is similar to Huang et al. (2010), which assumes that a mixture of snow contains only ice and air. The water fraction is not considered in Huang et al. (2010).

L263: "The particle size was" to 'Maximum particle size ranged from'

Reply: The sentence has been revised as per the reviewer’s suggestion. Please see Lines 276-277.

L279: Since there are many sites involved in this study, it could be useful to have a small map showing their locations.

Reply: This study is part of a series of studies of ICE-POP 2018. Many published papers contain such information. The authors would like to use references to provide such information to keep the manuscript concise. “The instruments were located in nineteen sites across the Gangwon region on the east coast of Korea (see Kim et al. 2021 for detailed information of each site).” Please Lines 93-94.

L315: "number density function" to 'number concentration'

Reply: The sentence has been revised as per the reviewer’s suggestion. Please see Lines 325-326.

L331: How is mean bulk density calculated here? Is it integrated over the total volume?

Reply: The mean bulk density is replaced by the median value of bulk density. The median value is obtained for each site. Please see Line 341.

L334: Since rain was not excluded from the retrievals, we are now talking about the mean bulk density of mixed precipitation instead of snow. As the densities of rain and snow are quite different, the mean value is easily driven by the fraction of rain, masking the possible signal from snow properties.

Reply: The number concentration of the retrieved bulk density is shown in Fig. 14. Both the numbers of the dry snow and mixing-phase events are shown in both warm-low and cold-low events. The median values of the retrieved bulk density of each site are shown in Fig. 14a,b. The temperature ($^{\circ}\text{C}$) and water vapor pressure (hPa) measurements from nearby mountain and coastal AWS sites are collected and summarized in Fig. 14e. The warm-low events have warmer and moister conditions compared to cold-low events. The warm- and cold-low events in the coastal area have similar mean temperature values. On the other hand, the water vapor pressure increases significantly from cold-low to warm-low events. The mountain area has similar features but with higher temperature increments and fewer increments of water vapor pressure. Please see Lines 339-357.

L345: This sentence seems to suggest that the density of snow has an impact on the weather. It's unclear to me what was meant here. Please rephrase to clarify.

Reply: The sentence has been revised. Please see Lines 419.

L526: "The Z_{HH} variation with v_w is much less than that with v_i ". I think, the opposite is true.

Reply: It should be "On the contours of Z_{HH} , the Z_{HH} variation with v_w is much less than that with v_i ." The sentence has been rephrased; please see Lines 628.

L560: What does the "shaded area" refer to in Fig. 5c?

Reply: The "shaded area" refers to the MRR reflectivity profile. The sentence has been revised to improve the clarity. "The time series of MRR Z_{HH} vertical profile (dBZ) from the third gate (0.45 km) to the 5 km." Please see Fig. 5 and 7-11.

Figures 5d, 9d-11d: There seem to be flat parts in the temperature measurements, where the measured value does not seem to change even for a fraction of a degree. These look like a measurement errors, perhaps gaps in the measurements. This raises concerns about the quality

of the temperature measurements. The measurements should be checked and erroneous values omitted from the analysis. If there is a cause for concern about the quality of the measurements, it should be discussed in the manuscript.

Reply: The temperature measurements were derived from collocated AWS (Vaisala WXT520). The comparison between the temperature measurements from AWS and Parsivel has shown that WXT520 has better performance. The Parsivel data had a significant bias in the Parsivel temperature data. The information on the temperature sensor has been added to the revised manuscript. The scale range of the temperature in Fig. 5, 7-11 is also improved for clarity.

Figure 6: The integration times in these figures are quite long. For example, in Fig. 6b, there seem to be multiple modes in the (D, v) distribution. Because of the long integration time, it is unclear if these modes are co-existing or if the dominating particle type is evolving over time. Have the authors considered analyzing the particle properties such as (D, v) distribution in shorter time intervals?

Reply: The authors did examine shorter time intervals for (D, v) distribution. The (D, v) distribution showed better differentiation between dry and mixing-phase snow. Both Fig. 6 and 12 can illustrate the transition of the mixing phase to dry snow. Considering the number of the figure and keeping the manuscript concise, we would like to maintain the current format of Fig. 6 and Fig. 12.

Technical comments

L10: Authors should choose between the spellings "disdrometer" and "distrometer". Currently, mixed spelling is used for this word in the manuscript.

Reply: The “distrometer” has been revised to “disdrometer”.

L27: Since riming refers to a process and not a hydrometeor type, change "riming" to 'rimed particles'.

Reply: The “riming” has been revised to “rimed particles”. Please see Line 27.

L73-74: The readability of this sentence could be improved by rephrasing.

Reply: Please see Lines 81-82. The sentence has been revised: Subsequently, the measurement of Z_{HH} weighted fall velocity (V_Z) from MRR is compared with the calculated V_Z from the derived bulk density and Parsivel PSD measurement.

L121: The authors probably meant 'modified FROM Huang et al. (2010)'.

Reply: The typo has been corrected. Please see Lines 138.

L142: "as the increasing" to 'with increasing'

Reply: The sentence has been revised as per the reviewer's suggestion. Please see Line 161.

L178: "examined with" to 'compared with'

Reply: The sentence has been revised as per the reviewer's suggestion. Please see Line 193.

L186: "four with Pluvio" to 'four of them equipped with a Pluvio'

Reply: The sentence has been revised as per the reviewer's suggestion. Please see Line 200.

L196: "consistency of" to 'consistent'

Reply: The sentence has been revised as per the reviewer's suggestion. Please see Line 209.

L232: Full stop after "shown in Fig. 5"

Reply: The sentence has been revised as per the reviewer's suggestion. Please see Line 347.

L267: "relatively weaker" to 'weaker'. There are also other instances of using "relatively" with a comparative in the manuscript. I advice against this.

Reply: The sentence has been revised as per the reviewer's suggestion. Please see Line 280. Other similar comparatives have been revised as well.

L274: "precipitation system" to 'precipitation'

Reply: The sentence has been revised as per the reviewer's suggestion. Please see Line 283.

L303: "has a more consistent relation" to 'is more consistent with the relation'

Reply: The sentence has been revised as per the reviewer's suggestion. Please see Line 314.

L345: "microphysics processes" to 'microphysical processes'

Reply: The sentence has been revised as per the reviewer's suggestion. Please see Line 419.

L353: "Consistency" to 'Inconsistency'

Reply: The sentence has been revised as per the reviewer's suggestion. Please see Line 425.

L361: The manuscript could be more consistent with how dates are written: with or without ordinal indicators.

Reply: The sentence has been revised as per the reviewer's suggestion. Please see Line 431.

L501: "blue lines" to 'blue', as there are also other symbols than lines.

Reply: The sentence has been revised as per the reviewer's suggestion. Please see Line 603.

L524: "DSD" to 'PSD'

Reply: The sentence has been revised as per the reviewer's suggestion. Please see Line 624.

L569: "derived" to 'shown'

Reply: The sentence has been revised as per the reviewer's suggestion. Please Line 669.

Figure 5d: "MRM" to 'MRR' in the y-axis label.

Reply: The typo has been corrected. Please see Fig. 5d.

Figure 6c: label (c) missing from figure

Reply: The typo has been corrected. Please see Fig. 6c.

Dear Reviewer,

The authors sincerely appreciate your valuable comments and suggestions to help improve the manuscript. We have revised the manuscript titled “Estimating the Snow Density using Collocated Parsivel and MRR Measurements: A Preliminary Study from ICE-POP 2017/2018 ”. that was submitted to ACP (Atmospheric Chemistry and Physics) on 3 January, 2024. Based on your suggestions, we have put substantial effort into additional analysis. The manuscript has been thoughtfully revised regarding the comments from all reviewers.

One of the major concerns of the proposed density retrieval algorithm using collocated MRR and Parsivel is lacking the uncertainty analysis. As per the reviewer’s suggestion, we have performed substantial investigations of the retrieval uncertainty. The impacts of the measurement uncertainty of the Parsivel and the MRR on the bulk density retrieval are analyzed quantitatively. The measurement issue of Parsivel is also investigated to understand its impact on bulk density retrieval. The results are summarized in the revised manuscript as a Discussion section.

The MRR data quality issue has been examined per the reviewer’s suggestion. The post-processed data have replaced the entire MRR raw data by applying the algorithm from Maahn and Kollias (2012). All the bulk density, bulk water fraction, and reflectivity-weighted velocity retrievals have been recalculated. The figures have been revised as well.

The original purpose of utilizing reflectivity-weighted velocity to filter adequate retrieval is no longer needed and has been removed in the revised manuscript. The quality of the retrieval results has been greatly improved by applying the post-processed MRR data per the reviewer’s suggestion. The low SNR MRR measurement has been removed. The comparison of reflectivity-weighted velocity is mainly used to identify the inadequate retrieval due to the attenuation effect on MRR reflectivity.

The performance of the retrieved bulk density has been validated by the snowfall rate (SR) from collocated Pluvio measurements and reflectivity-weighted fall velocity (V_z) from MRR. In addition to SR and V_z , the performance of the retrieved bulk density has been compared with the precipitation imaging package (PIP), a video disdrometer (Newman et al., 2009; Pettersen et al., 2020). The PIP was also deployed at the MHS site during ICE-POP 2018 (Tokay et al., 2023). The comparison of retrieved bulk density between the proposed algorithm in this study and PIP has shown good agreement with each other. The high consistency further confirms the performance of the retrieved bulk density. Since there is no direct bulk water fraction measurement for validation, the authors consider the validation of bulk density retrieval to PIP and Pluvio as “indirect” evidence to support the bulk water fraction retrieval.

The SR and Vz validation analysis shows that the algorithm can adequately retrieve the bulk density and bulk water fraction. The consistency of the retrieved bulk density to collocated PIP confirms the performance of the proposed algorithm in this study. The advantage of the proposed algorithm is that it utilizes collocated Parsivel and MRR, which are commercially available, commonly used, and robust instruments. The Parsivel and MRR can operate unattended and need little maintenance. Further application of the proposed algorithm helps derive long-term observation data on snow properties. The authors believe the proposed algorithm can provide an alternative choice if sophisticated instruments (e.g., 2DVD, PIP, SVI, MASC) are unavailable.

The manuscript has also been revised carefully following the reviewer's suggestions on English wording. The authors would like to express our sincere appreciation for the comments. The added or modified sentences in the revised manual are in red for your convenience.

The point-to-point replies to every comment have been prepared in the following. For your convenience, the reply is arranged as follows,

Reviewer's comments

Response

Revisions in the manuscript

We would appreciate any feedback on the revisions.

General Comments #####

1. High sensitivity of Z_{HH} to the liquid portion of the particle allows for precise bulk water fraction estimation.

The study provides no evidence that the bulk water (liquid) fraction produced by the retrieval is consistent with actual bulk liquid water fraction. The claim that the retrieval can estimate bulk liquid water fraction is supported only by a brief argument regarding the differing sensitivity of the retrieval forward model to the water and ice volume fractions.

Reply: The bulk water fraction is derived along with the maximum possible bulk density in the proposed method in this study. If a different assumption is made when selecting possible bulk density, the retrieved bulk water fraction will be different. Therefore, the

performance of the retrieved bulk water fraction is linked with bulk density retrieval. Since there is no direct measurement of bulk water fraction, we compare the retrieved bulk density from the proposed method and PIP. The consistency between retrieved bulk density from the two algorithms strengthens the reliability of the retrieved bulk water, which should be reasonable. Please see Figure R1.

As shown in Fig. R1(a), the retrieved bulk density values from the proposed algorithm and PIP gradually decrease from nearly 1.0 to 0.1 (g cm^{-3}) between 03 and 06 UTC. Both algorithms capture the transition from the mixing-phase to dry snow.

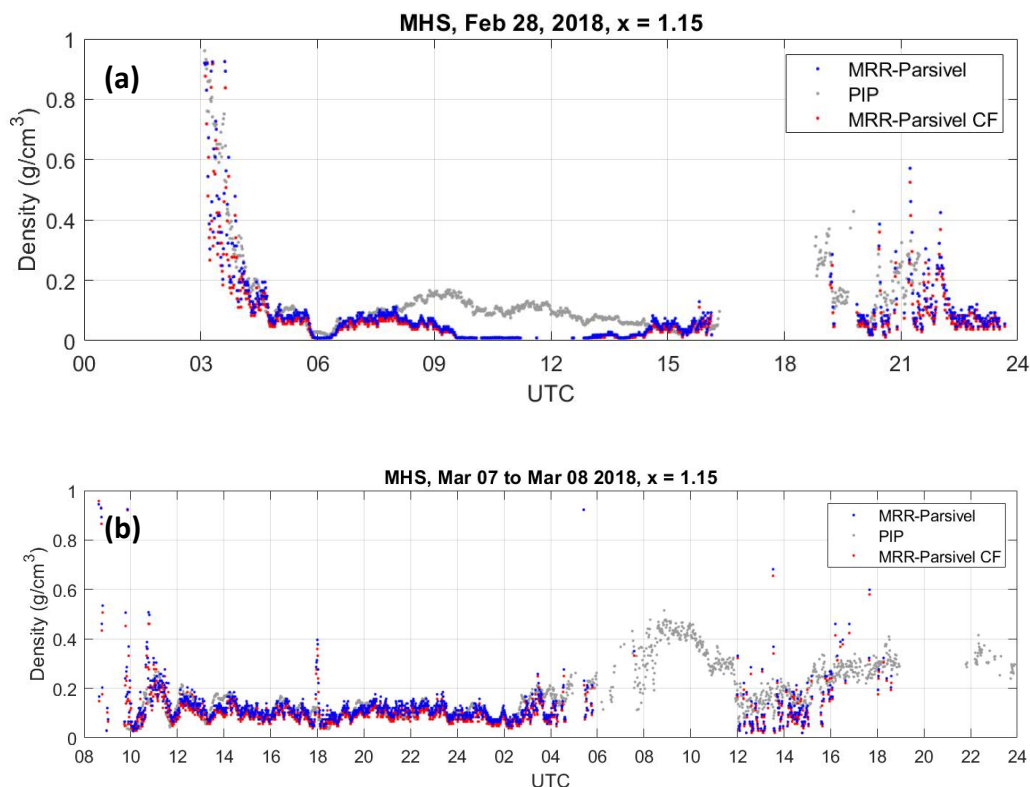


Figure R1: (a) The retrieved bulk density from collocated MRR and Parsivel. The blue dots are retrieved from CF-adjusted PSD. The red dots are from the original PSD. The gray dots are the retrieval from PIP. The case is 28 February 2018. (b) Same as (a), but for case 7 March 2018.

The manuscript has been revised to include the discussion of the bulk water fraction retrieval. **Please see Lines 398-413 in the revised manuscript. Or see the following.**

5.3 The bulk density comparison with collocated PIP

The precipitation imaging package (PIP), a video disdrometer, provides the PSD, fall speed, density, and snowfall rate of hydrometers (Newman et al., 2009; Pettersen et al., 2020) was

also deployed at the MHS site during ICE-POP 2018. Tokay et al. (2023) have utilized PIP to investigate the PSD parameters, including mass-weighted diameter and normalized intercept. The bulk density is estimated by Tokay et al. (2023) with various assumptions. The PIP retrieved density was generated from the assumption that $D_{\max} = 1.15 D_{\text{eq}}$, and the mass derivation included was based on Bohm (1989). As shown in Fig. 15, the retrieved bulk density from the proposed algorithm in this study and PIP have high consistency. Both retrieved bulk densities are highly correlated to each other, except for the period of 08 to 15UTC on 28 February due to the attenuation effect of the accumulated snow on the MRR antenna (Fig. 5e).

The bulk water fraction is derived along with the maximum possible bulk density using the proposed method in this study. The retrieved bulk water fraction will differ if a different assumption is made when selecting possible bulk density. Therefore, the performance of the retrieved bulk water fraction is linked with bulk density retrieval. Since there are no direct measurements of bulk water fraction, the consistency between retrieved bulk density from two algorithms “indirectly” confirms that the retrieved bulk water should be reasonable. As shown in Fig. 15a, the retrieved bulk density values from the proposed algorithm and PIP gradually decrease from nearly 1.0 to 0.1 (g cm^{-3}) between 03 and 06 UTC. Both algorithms capture the fast transition from the mixing-phase to dry snow.

Despite the various possible factors that can degrade the performance of bulk density retrieval from collocated MRR and Parsivel, the uncertainty study has shown that the retrieval performance has an acceptable low impact by the Parsivel and MRR observational error. The agreement between this study and PIP retrieval further confirms that the proposed algorithm can robustly retrieve the bulk density and water fraction from collocated MRR and Parsivel.

2. The use of Vz as a filter improves agreement between measured snowfall rates and snowfall rates estimated from the bulk-density retrievals.

Again, this isn't supported. The study describes retrieval performance using only data to which the filter has already been applied. It does not show retrieval results when the filter is not applied, so no judgement can be made about the effects of the filter.

Reply: We did calculate the SR before and after the Vz filter, and the results did show great improvements. As per the reviewer's suggestion regarding the data quality of MRR, the MRR data has been replaced by the post-processed data, which has been applied to the algorithm by Maahn and Kollias (2012). All the bulk density, bulk water fraction, and reflectivity-weighted velocity retrievals have been recalculated. The original noisy retrieval results have been removed due to low SNR. The Vz calculation is no longer used to remove noisy bulk density retrieval. The Vz comparison is derived to verify the overall performance of bulk density retrieval. In addition, the Vz can identify the inadequate

bulk density retrieval due to the attenuation effect on MRR reflectivity. Please see Lines 185-187 in the revised manuscript. Or see the following.

The comparison of V_Z^{MRR} and $V_Z^{\rho_{bulk}}$ is considered an overall validation of the retrieved bulk density. In addition, the inconsistency between the $V_Z^{\rho_{bulk}}$ and the V_Z^{MRR} can identify inadequate bulk density retrieval. For example, the attenuation effect can lead to underestimating the MRR reflectivity measurement and, thus, underestimating the retrieved bulk density.

3. Microphysical similarity between two warm low synoptic events confirms the dependence of the micro-scale factors on the synoptic conditions.

The results from the study show similarities in the retrieved microphysical properties for these two events, but that is not sufficient to support the conclusion. Perhaps other synoptic setups would produce similar microphysical properties, negating this conclusion.

Reply: The warm-low events (28 February 2018 and 7 March 2018) shown in the manuscripts are the events that have the most accumulated snowfall during ICE-POP. The 28 February case demonstrates that the retrieved snow density is reasonable compared to Pluvio SR. However, some discrepancies between the calculated V_z from retrieved bulk density and measurements of V_z from MRR can be noticed. The discrepancy is due to the attenuation effect on the MRR antenna. The authors do not intend to emphasize the similarity of microphysical properties. These two events are selected to demonstrate the evolution of the bulk density retrieval results in detail. The discussion has been revised. Please see Lines 339-357 in the revised manuscript. Or see the following.

To further understand the microphysical characteristics of winter precipitation, each site's retrieved bulk density and bulk water fractions are divided into warm-low (nine cases) and cold-low (five cases) events according to the synoptic condition (Gehring et al. 2020; Kim et al. 2021). As shown in Fig. 14a, the median values of bulk density of warm-low events from the mountain site (YPO) to the coastal site (GWU) are about 0.10 to 0.29 g cm⁻³. The GWU site has the highest bulk density. On the other hand, the median values of bulk density of cold-low events from YPO to GWU are about 0.07 to 0.05 g cm⁻³ (Fig. 14b). The overall bulk density values are lower in cold-low events than in warm-low events.

In Fig. 14c and d, more than 90% of bulk water fractions are less than 0.03 for warm- and cold-low events. The YPO site has the lowest bulk water fraction, especially the cold-low events that remain lower than 0.22. The mean value of the top 5% of the bulk water fraction of each site is obtained for further investigation. The values of bulk water fraction gradually increase from the mountain site (YPO) to the coastal site (GWU) for both warm- and cold-low

events. The mean values of the top 5% bulk water fraction of YPO, MHS, and CPO sites for warm-low events are 0.0015, and the BKC and GWU are about 0.32 to 0.45. The cold-low events are 0.0013 to 0.19 for each site.

The temperature ($^{\circ}\text{C}$) and water vapor pressure (hPa) measurements from nearby mountain and coastal AWS sites are collected and summarized in Fig. 14e. Warm-low events have warmer and moister conditions than cold-low events. The coastal area's warm- and cold-low events have similar mean temperature values. On the other hand, the water vapor pressure increases significantly from cold-low to warm-low events in the coastal region. The mountain area has similar features, but higher temperature increments and fewer increments of water vapor pressure. These results indicate that the winter precipitation systems of coastal sites with warmer and moister environments have higher bulk density and bulk water fraction than mountain sites.

4. Differences in bulk density and water fraction between mountain sites and coastal sites are indicative of geographical and synoptic environmental effects on the distinct microphysical characteristics of winter precipitation systems.

The geographical effects are suggested somewhat by the results from the second case study, but as noted in regards to conclusion #3, synoptic control can't be demonstrated using two cases with similar synoptic setup. Further, although the authors discuss differing meteorological properties at the coastal and mountain locations, there is no demonstration that the coastal and mountain sites differ in moisture availability.

Reply: The number concentration of the retrieved bulk density is shown in Fig. 14. Both dry snow and mixing-phase events are shown in both warm-low and cold-low events. The median values of the retrieved bulk density of each site are shown in Fig. 14a,b. The temperature ($^{\circ}\text{C}$) and water vapor pressure (hPa) measurements from nearby mountain and coastal AWS sites are collected and summarized in Fig. 14e. The warm-low events have warmer and moister conditions compared to cold-low events. The coastal area's warm- and cold-low events have similar mean temperature values. On the other hand, the water vapor pressure increases significantly from cold-low to warm-low events. The mountain area has similar features but with higher temperature increments and fewer increments of water vapor pressure. Please see Lines 339-357 of the revised manuscript. Or see the previous reply.

A. There are no estimates of retrieval uncertainties. This makes it impossible to determine, for example, if differences between the observed and retrieval-derived snowfall rates are significant.

Reply: The retrieval uncertainty is investigated as per the reviewer's suggestion. The retrieval uncertainty analysis is performed by considering the assumption of particle shape, Parsivel measurement uncertainty, and the MRR measurement uncertainty. The detailed retrieval uncertainty analysis has been summarized in the newly added Discussion section. Please see Lines 358-417 in the revised manuscript. Or see the following.

5 Discussion

The proposed retrieval algorithm has shown that it can estimate the bulk density and bulk water fraction with reasonable performance. The underestimation of retrievals caused by the attenuation effect of MRR reflectivity can be well identified by reflectivity-weighted velocity. In addition to the attenuation effect, the uncertainties of the retrieval algorithm can be attributed to observational data quality and the algorithm's basic assumption. In the following discussion, Parsivel's PSD measurement uncertainty will be investigated. In addition, the impact of bulk density and water fraction retrieval from spherical particle assumption and the uncertainty of MRR reflectivity measurement will be discussed.

5.1 The measurement uncertainty of Parsivel fall velocity and its impact on the bulk density and water fraction retrieval

As indicated by the study by Battaglia et al. (2010) and Wood et al. (2013), Parsivel's fall velocity measurement may not be accurate for a snowflake particle. This issue is due to the internally assumed relationship between horizontal and vertical snow particle dimensions. Yuter et al. (2006), Aikins et al. (2016), and Kim et al. (2021) indicate the splashing and border effects of the diameter of < 1 mm in Parsivel fall velocity measurements. The fall velocity issue explains why the consistently high fall velocity of diameter less than 1 mm in the MHS site can be noticed by the fall velocity-diameter relation in Figs. 6 and 12; even the retrieved bulk density and water fraction were low and should be associated with low fall velocity. Yuter et al. (2006) and Aikins et al. (2016) suggest a quality control procedure that discards particles with a diameter of < 1 mm to avoid splashing and border effects.

As Battaglia et al. (2010) indicated, the Parsivel overestimates the snowfall velocity and underestimates the PSD. A correction factor (CF) derived from comparing the collocated 2DVD in the MHS site is suggested by Dr. Gyuwon Lee (personal communication). The particle size-dependent CF adjusts the fall velocity measurement from Parsivel and thus modifies the PSD. The CF reduces the fall velocity to a factor of two as the particle size is around 10 μ m. The modified PSD has a higher concentration after applying CF adjustment. The bulk density and water fraction retrieval uncertainty due to PSD measurement issues are investigated using the PSD and CF-adjusted PSD. As shown in Fig. 15, the bulk density

retrieval decreases slightly after applying CF-adjusted PSD in the 28 February and the 7 March 2018 events. The bias of retrieved bulk density is about -0.0153 (g cm^{-3}), and the standard deviation is about 0.095 (g cm^{-3}). The bias and the standard deviation for bulk water fraction - 1.8×10^{-4} and 2.6×10^{-3} .

The results indicate that with the measurement uncertainty of PSD from Parsivel, the bulk density and water fraction retrieval are fairly low. It is postulated that fall velocity measurement uncertainty slightly impacts the PSD calculation; thus, the bulk density and water fraction retrieval uncertainty is sufficiently low.

5.2 The measurement uncertainty of MRR reflectivity and its impact on the bulk density and water fraction retrieval

The simulation of MRR reflectivity can be sensitive to the particle shape assumption. A sensitivity investigation assuming the particle axis ratio of 0.5 shows that about 1.5 dBZ variation of MRR reflectivity can be induced. Another possible source of retrieval uncertainty is the measurement of MRR reflectivity. As discussed in the MRR bias calculation from pure rain events, the standard deviation between MRR reflectivity and Parsivel calculated reflectivity is about 1.1 to 1.3 dBZ for each site. A random error of MRR reflectivity with a standard deviation of 1.2 dB is introduced into the retrieval algorithm to imitate the particle assumption and MRR measurement uncertainty. In Figure 16(a), the algorithm overestimates the bulk density ($\Delta\rho^{bulk} > 0$) as the MRR reflectivity's positive error ($\Delta Z_{HH} > 0$) increases. On the other hand, the negative bias of MRR reflectivity ($\Delta Z_{HH} < 0$) led to an underestimation of the bulk density retrieval ($\Delta\rho^{bulk} < 0$). The overall standard deviation of bulk density retrieval uncertainty is about 0.025 (g cm^{-3}) for a given MRR reflectivity uncertainty of 1.2 dB. The bulk water fraction retrieval has the same feature shown in Fig. 16(b). Given an MRR reflectivity uncertainty of 1.2 dB, the bulk water fraction retrieval uncertainty is about 0.041.

5.3 The bulk density comparison with collocated PIP

The precipitation imaging package (PIP), a video disdrometer, provides the PSD, fall speed, density, and snowfall rate of hydrometers (Newman et al., 2009; Pettersen et al., 2020) was also deployed at the MHS site during ICE-POP 2018. Tokay et al. (2023) have utilized PIP to investigate the PSD parameters, including mass-weighted diameter and normalized intercept. The bulk density is estimated by Tokay et al. (2023) with various assumptions. The PIP retrieved density was generated from the assumption that $D_{max} = 1.15 D_{eq}$, and the mass derivation included was based on Bohm (1989). As shown in Fig. 15, the retrieved bulk density from the proposed algorithm in this study and PIP have high consistency. Both retrieved bulk densities are highly correlated to each other, except for the period of 08 to 15UTC on 28

February due to the attenuation effect of the accumulated snow on the MRR antenna (Fig. 5e).

The bulk water fraction is derived along with the maximum possible bulk density using the proposed method in this study. The retrieved bulk water fraction will differ if a different assumption is made when selecting possible bulk density. Therefore, the performance of the retrieved bulk water fraction is linked with bulk density retrieval. Since there are no direct measurements of bulk water fraction, the consistency between retrieved bulk density from two algorithms “indirectly” confirms that the retrieved bulk water should be reasonable. As shown in Fig. 15a, the retrieved bulk density values from the proposed algorithm and PIP gradually decrease from nearly 1.0 to 0.1 (g cm^{-3}) between 03 and 06 UTC. Both algorithms capture the fast transition from the mixing-phase to dry snow.

Despite the various possible factors that can degrade the performance of bulk density retrieval from collocated MRR and Parsivel, the uncertainty study has shown that the retrieval performance has an acceptable low impact by the Parsivel and MRR observational error. The agreement between this study and PIP retrieval further confirms that the proposed algorithm can robustly retrieve the bulk density and water fraction from collocated MRR and Parsivel.

B. The description of the methodology is not sufficient. For example, a Rayleigh reflectivity model is described, but that is not what is used in the radar forward model. Also, the description of how the ice and liquid volume fractions are determined in the retrieval is unclear and not well justified.

Reply: The description of the methodology has been improved per the reviewer’s suggestion. The description of the reflectivity calculation has been revised to improve the clarity. The equation 2 is no longer the Rayleigh reflectivity model. The backscattering cross-section (σ) replaces D^6 in equation 2. The reference of Bringi and Chandrasekar (2001) is provided to replace Huang et al. (2010). The ice and water are assumed to be evenly distributed within the particle. Please see Lines 125-171 of the revised manuscript. Or see the following.

3 Methodology

Hydrometeor is composed of particles with combinations of solid ice and liquid water with a density of 0.92 (ρ_{ice}) and 1.0 (ρ_{water}) g cm^{-3} , respectively. Therefore, the hydrometeor bulk density (ρ_{bulk}) can be determined by its volume ratio of solid ice (v_i) and liquid water (v_w) as follows,

$$\rho_{bulk} = v_i \times 0.92 + v_w; \text{ g cm}^{-3}. \quad (1)$$

The sum of the values of v_i and v_w equals one or less than one if it contains air in the particle. Thus, the reflectivity factor (Z_{HH}) can be calculated as follows (Bringi and Chandrasekar 2001),

$$Z_{HH} = \left(\frac{\rho_{bulk}}{\rho_{ice}} \right)^2 \frac{|K_{ice}|^2 \lambda^4}{|K_w|^2 \pi^5} \int \sigma(D) N(D) dD; mm^6 m^{-3}. \quad (2)$$

The K_{ice} and K_w are the dielectric factors of solid ice and liquid water, respectively. σ is the backscattering cross-section, D is the particle size, and $N(D)$ is the particle size distribution. As shown in (1) and (2), the Z_{HH} is positively correlated to ρ_{bulk} . The higher hydrometeor bulk density has a higher value of Z_{HH} for a given PSD. Hence, the Z_{HH} , the factor relating to the v_i and v_w of hydrometeor, can estimate the bulk density. Huang et al. (2010) utilized the C-band radar measurements on top of a 2DVD. The ρ_{bulk} was derived from (2) by applying the reflectivity from scanning C-band radar and the PSD from 2DVD.

The bulk density estimation algorithm developed in this study is modified from Huang et al. (2010). Instead of scanning C-band radar and 2DVD, the collocated MRR (Micro Rain Radar, Löffler-Mang et al. 1999) and Parsivel are proposed to minimize the sampling size inconsistency. The estimated density is considered as "bulk" or "equivalent" density since the MRR Z_{HH} measurement is the summation of all hydrometeor within the sampling volume. The procedures of the proposed method are introduced in the following section, and the validation and discussion are described in the next section.

The Z_{HH} values were simulated from each Parsivel PSD measurement. Each Z_{HH} value was calculated using a rigorous T-matrix method with specified v_i and v_w (Vivekanandan et al. 1991; Bringi and Chandrasekar 2001). The ice and water are assumed to be evenly distributed within the particle. The T-matrix method is a fast numerical solution of Maxwell's equations to compute the scattering properties of particles. The shape of the hydrometeor is regarded as a symmetric sphere since the Z_{HH} measurement of the hydrometer was observed from the bottom of the snow particle by vertical pointing MRR. The mean and standard deviation of the canting angle are assumed 0° and 20° , respectively. The sensitivity of the particle shape to bulk density retrieval will be investigated in the discussion section.

An example of simulated Z_{HH} from Parsivel observed snow PSD via T-matrix simulation with different combination of v_i/v_w and temperature is shown in Fig. 1. The results indicate that the simulated Z_{HH} values remain nearly identical when varying the temperature from -10 to 0°C . On the other hand, the simulated Z_{HH} varies significantly when altering the composition of v_i/v_w . The lowest (highest) value of Z_{HH} was from the combination of v_i/v_w of $1.0/0.0$ ($0.0/1.0$), which was pure ice (rain) with a density of 0.92 (1.0) g cm^{-3} . The particle temperature was consequently assumed to have a constant value of 0°C in the following Z_{HH} T-matrix simulation. On the other hand, all possible combinations of v_i and v_w ranging from 0.0 to 1.0 were included in the T-matrix simulation of Z_{HH} .

A selected example of the simulated Z_{HH} from observed PSD with various combinations of v_i/v_w is shown in Figure 2. The observed PSD from Parsivel (Fig. 2a) was applied to the T-Matrix backscattering simulation. All possible combinations of v_i/v_w were applied to calculate simulated Z_{HH} (Fig. 2b). The corresponding bulk density was derived via (1) and shown as

contour dash lines in Fig. 2b. The values of simulated Z_{HH} vary from 0 to 50 dBZ (shaded color in Fig. 2b). The simulated Z_{HH} values increase with increasing of the bulk snow density. In this selected case, the observed Z_{HH} from MRR was 22.23 dBZ (dashed blue line in Fig. 2b). The observed Z_{HH} from MRR was thus applied to constrain the possible combination of v_i/v_w and bulk density. The possible ranges of v_i/v_w are 0.0/0.009 to 0.08/0.0, shown as a dashed blue line in Fig. 2b. The corresponding bulk densities are 0.009 and 0.074 (g cm^{-3}), respectively. The higher the fraction of ice (e.g., v_i), the higher bulk snow density values can be found in Fig. 2b. To determine the bulk snow density from possible combinations of v_i/v_w , the maximum bulk density with maximum v_i is selected. Choosing the bulk density with maximum v_i ensures the minimum value of v_w . This assumption is similar to Huang et al. (2010), which assumes that a mixture of snow contains only ice and air. The water fraction is not considered in Huang et al. (2010). Therefore, the contour's maximum density in Fig. 2(b), 0.074 g cm^{-3} , is determined by assuming v_i and v_w are 0.08 and 0.0, respectively. Subsequently, the v_w is regarded as "bulk water fraction," which can also be estimated in the proposed method, in addition to the bulk density, and will be analyzed in the following section.

C. The reflectivity and Doppler velocity data from the MRR require reprocessing to be representative of snowfall. See Maahn and Kollias (2012). It's not clear if this or similar reprocessing was performed.

Reply: The MRR data has been post-processed per the reviewer's suggestion. The values of bulk density and bulk water fraction have been recalculated. The impact of the Z_{HH} difference on the values of bulk density and bulk water fraction can be considered as the retrieval uncertainty due to MRR reflectivity measurement uncertainty. The results are shown in the Discussion section. Please see Lines 111-114 in the revised manuscript. Or see the following.

The MRRs had the same configuration during ICEP-POP; the vertical resolution was 150 m, and there were 31 gates up to 4.65 km. The MRR data was post-processed using the algorithm from Maahn and Kollias (2012). The sensitivity of MRR has been enhanced, and the Doppler velocity has been dealiased. The third gate (450 m above ground) of Z_{HH} data from MRR was selected to retrieve snow density since the first two gates contain some clutter contamination.

D. The discussion of results, particularly for the 7-8 March 2018 case, needs to be better organized and cleaned up to more clearly bring focus to the significant patterns in the results.

Reply: The discussion of the 7-8 March 2018 case has been rewritten to improve the clarity. Please see Lines 278-322 in the revised manuscript. Or see the following.

4.4 Case study: 7 March 2018

Both the 7 March and 28 February events share similar larger-scale conditions. The difference between these two events is that the precipitation on the 7 March was weaker yet persisted for a longer time than the 28 February event. An east-moving trough from east China became a potential vorticity streamer (Gehring et al. 2020). The low-pressure system developed over the Korean peninsula and produced intensive precipitation. Besides the similarity in larger-scale conditions, the microphysical characteristics of precipitation systems share similar behaviors in these two cases. The intensive precipitation associated with the low-pressure system started at 10 UTC on 7 March. As the nimbostratus weakened and dissipated into the shallow convection at about 03 UTC on 08 March 2018, the high bulk density can be found in most sites (Fig. 8a-11a). The weakened precipitation with shallow convections can be seen from 08 UTC to 19 UTC on 8 March (reflectivity profiles in Fig. 7c-11c).

The overall bulk density and bulk water fraction in the GWU site (Fig. 11) are the highest in all sites. In contrast, the YPO (Fig. 7) site demonstrates a relatively lower magnitude of bulk density and bulk water fraction, especially after 04 UTC on 8 March. The contrast may be attributed to their environmental condition, as the YPO site is located in the westernmost mountainous area of the five sites. In contrast, the GWU site is located on the east coast, which faces abundant moisture from the East Sea (Kim et al. 2021). Gradual increase of density, as well as the bulk water fraction, can also be found in the distribution of fall velocity versus the diameter from MHS, BKC, to the GWU sites (Fig. 12). The GWU site features mostly the particles concentrated around the fall velocity-diameter relation of rain. Meanwhile, in MHS and BKC sites, especially the MHS site, data are distributed more discretely and scattered between the relation of rain and the relation of dry dendrites. Overall, the retrieved bulk density and bulk water fraction successfully reveal distinct fall velocity-diameter relations of each site due to the different synoptic environments.

The YPO, MHS, and CPO sites had continual low bulk density and bulk water fraction values (about 0.1 to 0.2 g cm⁻³, Figs. 7a-9a) at the beginning of the precipitation. The MRR reflectivity profiles indicate an intensive precipitation system up to 5 km (Figs. 7c-9c) from 10 UTC on 7 March to 04 UTC on 8 March. The precipitation gradually dissipated at 04 UTC on 8 March. The PSD was featured with large particle size (Figs. 7b-9b) and aggregates-like particles (Gehring et al. 2020). On the other hand, the coastal sites (BKC and GWU) began with nimbostratus cloud and high values of bulk density and bulk water fraction, 10 to 13 UTC for BKC and 10 to 19 UTC for GWU on 7 March (Figs. 10a,b and 11a,b). The high bulk density (about 0.9 g cm⁻³) period corresponds to a higher bulk water fraction from 0.4 to 0.8. The precipitation gradually transited to a low bulk density as other sites (YPO, MHS, and CPO) till 04 UTC on 8 March. The fall velocity-diameter relation confirms the high bulk water fraction. The Parsivel data reveals the fall velocity-diameter relation of rain from 08 to 19 UTC on 7 March (Fig. 12c), and the graupel relation from 19 UTC to 03 UTC on 8 March in the GWU site (Fig. 12f). The higher density initially in MHS and BKC sites are also confirmed by the

same contrast between 08 to 19 UTC on 7 March (Figs. 12a, b) than 19 UTC to 03 UTC on 8 March (Figs. 12d, e).

After 04 UTC on 8 March, the BKC and GWU sites featured high bulk density and bulk water fraction (Figs. 10a-11a). The PSDs were mainly small particles (Figs. 10b-11b). According to MRR measurements, the precipitation systems were weaker and shallower (Figs. 10c-11c) compared to the period with low bulk density before 04 UTC on 8 March. The V_z of particles also transitioned from consistently low values to slightly higher and more noisy values (Figs. 10e-11e), suggesting high-density particles with high fall velocity. Compared to 19 UTC on 7 March to 03 UTC on 8 March (Figs. 12d, e, and f), the fall velocity-diameter relation from 04 to 12 UTC on 8 March is more consistent with the relation of rain (Figs. 12g, h, and i). After 12 UTC, more particles were distributed between the relation of rain and graupel (Fig. 12j, k, and l).

Moreover, the good agreements between the Pluvio SR and the derived SR calculated from all sites' bulk density can be noticed in Figs. 7f-8f, and 10f-11f. The Pluvio is not available at the CPO site. Two distinct types of precipitation structures (according to MRR) and microphysical characteristics (bulk density, bulk water fraction, PSD) can be noticed in Figs. 7-11. One has deeper and more intensive precipitation structures, higher bulk density, and bulk water fraction, and it contains smaller particles. Overall, the estimation of the bulk density and the bulk water fraction demonstrates the contrast between sites of geographical locations and captures the evolution of the precipitation system. The statistical analysis of retrieved properties of mountain and coastal sites will be discussed in the following section.

E. There are assumptions of spherical particles in both the particle scattering calculations and in the fallspeed calculations, but only limited discussion of whether they are adequate for use with snowflakes and at the MRR's frequency.

Reply: The discussion of non-spherical particles has been introduced in the revised manuscript. Non-spherical and spherical particle measurements are different when MRR looks upward. However, the orientation of the non-spherical particle is assumed to be isotropic and homogeneous. A sensitivity investigation assuming the particle axis ratio of 0.5 has been conducted. The results show that about 1.5 dBZ variation of simulated reflectivity can be induced due to the assumption of particle size.

A random error of MRR reflectivity with a standard deviation of 1.2 dB is introduced into the retrieval algorithm to imitate the particle assumption and MRR measurement uncertainty. The overall standard deviation of bulk density retrieval uncertainty is about $0.025 \text{ (g cm}^{-3}\text{)}$ for a given MRR reflectivity uncertainty of 1.2 dB. The bulk water fraction retrieval has the same feature, and the uncertainty is about 0.041.

Please see the Discussion section (Lines 358-417) in the revised manuscript. Or see the reply to "comment A" shown previously, pages 7-9.

F. The particle "size" measured by the Parsivel is ill-defined for snow particles. For background, in addition to Battaglia et al., see also Wood et al. (2013). This makes it difficult to make useful comparisons of bulk particle densities that are determined using different types of disdrometer measurements (e.g., Figure 13).

Reply: In Figure 13, the bulk density comparison among this study, Heymsfield et al. (2004), and Brandes et al. (2007) does not intend to emphasize the difference. We convert D_0 to D_m by assuming exponential PSD ($D_m = D_0^{4/3.67}$). Considering distinct environmental conditions, instrumentations, and retrieval techniques, most of the particles in this study are consistent with the $\rho_{bulk} - D_m$ relation from Heymsfield et al. (2004) and Brandes et al. (2007). These results indicate that the proposed bulk density estimation algorithm can derive accurate retrievals with statistically consistent microphysical characteristics from previous studies. Please see Lines 324-338 in the revised manuscript. Or see the following.

The retrieved bulk density and bulk water fraction are investigated statistically to understand the microphysical characteristics of the winter precipitation systems from ICE-POP 2018 and its pre-campaign. Fig. 13 shows the number concentration of retrieved bulk density and observed mass-weighted diameter (D_m) from PSD of all sites. The bulk density decreases exponentially as D_m increases. Heymsfield et al. (2004) utilized the aircraft data collected from two field programs, namely the Atmospheric Radiation Measurement (ARM) program, Cirrus Regional Study of Tropical Anvils and Cirrus Layers (CRYSTAL) Florida Area Cirrus Experiment (FACE) in southern Florida during July 2002. The ARM data is mostly ice clouds formed primarily through large-scale ascent, and the CRYSTAL observations are mainly from convectively generated cirrus anvils. Brandes et al. (2007) utilized the data of 52 storm days from the Front Range in eastern Colorado during October–April 2003 to 2005 of a ground-based 2DVD. The data of Brandes et al. (2007) is dominated by almost spherical aggregates having near-exponential or superexponential size distributions. The $\rho_{bulk} - D_0$ relation (D_0 , median volume diameter) from Brandes et al. (2007) is replaced by D_m in Fig. 13 for comparison, assuming the exponential PSD and $D_m = 4D_0/3.67$.

Despite distinct environmental conditions, instrumentations, and retrieval techniques, most of the particles in this study are consistent with the $\rho_{bulk} - D_m$ relation from Heymsfield et al. (2004) and Brandes et al. (2007). These results indicate that the proposed bulk density estimation algorithm can derive reasonable retrievals with statistically consistent microphysical characteristics from previous studies.

F. In further revision, English-language usage and grammar could be improved. I have tried to include some comments in the details below that may be helpful.

Reply: Authors sincerely appreciate the reviewer's help. We have made all the corrections per both reviewers' suggestions. We will further improve the manuscript by asking for professional assistance from the English editor.

Line-by-line comments: #####

Abstract *****

L9: Does "bulk water fraction" mean bulk *liquid* water fraction? And is this the volume fraction or mass fraction?

Also, here and in other places, be careful how you use words to describe what you are retrieving. Here you say "hydrometeor's bulk density and bulk water fraction". This implies you are retrieving these properties for individual particles, which is not correct. You are retrieving the bulk density and bulk water fraction for populations of particles.

Reply: The sentence has been revised to improve the clarity. "derive bulk density and bulk water fraction of a population of particles ...". Please see Line 9.

The bulk water fraction is the volume fraction, not the mass fraction. Please see Lines 126-128 in the revised manuscript. Or see the following.

Hydrometeor is composed of particles with combinations of solid ice and liquid water with a density of 0.92 (ρ_{ice}) and 1.0 (ρ_{water}) g cm⁻³, respectively. Therefore, the hydrometeor bulk density (ρ_{bulk}) can be determined by its volume ratio of solid ice (v_i) and liquid water (v_w) as follows,

L13: The meaning of "The combination of minimum water fraction subsequently determines the bulk density" is not clear.

Reply: The sentence has been revised to improve the clarity. "The combination of minimum water fraction and maximum ice fraction subsequently determines the bulk density (ρ_{bulk})." Please see Lines 13-14 in the revised manuscript.

L15-16: The meaning of "self-evaluation" in this context is not clear. L20-21: Regarding "a similar transition", from what state to what state?

Reply: The “self-evaluation” has been removed in the revised manuscript. “The estimated ρ_{bulk} was examined independently by comparison of the liquid-equivalent snowfall rate (SR) of collocated Pluvio.” Please see Lines 15-16 in the revised manuscript.

L21: Again, you are retrieving population properties, not the properties of individual particles.

Reply: The sentence has been revised to improve the clarity. Please see Lines 21-22.

L28: Do you actually mean "liquid water content" here, which usually means the concentration (e.g., grams per cubic meter) of liquid water?

Reply: Yes, the authors refer to liquid water content (LWC, g cm⁻³). The LWC has been constantly retrieved by dual-polarimetric radar measurements.

Introduction *****

L30-31: This doesn't seem to be an example of either of the prior two statements in this section. What is it intended to exemplify?

Reply: The examples intend to show how microphysical parameterizations in numerical forecast models can be improved by validating with the snow property obtained from observational data. The sentence has been revised to improve the clarity. Please see Lines 33-44 in the revised manuscript. Or see the following.

These physical properties, including terminal fall speed, shape, composition, and density, are also crucial to verifying and improving microphysical parameterizations in numerical forecast models (Yuter et al., 2006; Kim et al., 2021). Simulating proper riming, freezing, and aggregation processes is challenging in numerical models. The riming processes led to snowfall velocity and density diversity in the same particle diameter size (Zhang et al. 2021). The supercooled liquid water freezes on snow particles and fills in the holes of snow; therefore, snow's mass and fall velocity increase while size has little changes (Heymsfield 1982; Moisseev et al. 2018). On the other hand, the melting process induces higher fall velocity and density by the aerodynamics process in a warm environment. The dispersed fall velocity caused by particles melted from dry snow to rain leads to higher collision efficiency and facilitates the aggregation and accretion processes (Yuter et al. 2006). Higher snow density is associated with steeper fall velocity-diameter (V-D) relations, which result from stronger riming (Lee et al. 2015) or melting processes (Yuter et al. 2006). To emulate the diverse physical properties of hydrometers, Morrison and Milbrandt (2015) proposed a new bulk method to parameterize ice-phase particles with evolvable density to study the role of density in numerical simulation. A

robust density estimation algorithm can evaluate microphysical simulations from numerical models.

L33-34: It's not specifically the increase in liquid phase fraction that causes the fallspeed of an individual particle to increase. It is the change in particle aerodynamics, specifically the reduction in particle size and horizontally-projected area while particle mass stays constant) that causes the fallspeed to increase.

Reply: The sentence has been revised as per the reviewer's suggestion. "On the other hand, the melting process in a warm environment induces higher fall velocity and density by the aerodynamics process." Please see Lines 38-39.

L38-39: It is not clear what point the authors are making with this statement. How is the work by Morrison and Milbrandt important to this work?

Reply: The study from Morrison and Milbrandt (2015) proposed a new microphysical scheme that parameterizes the density of hydrometers. A robust density estimation algorithm can evaluate microphysical simulations from numerical models. Please see the revised manuscript, Line 44.

L40: I think that "inhibits" is not the correct word here.

Reply: The typo has been corrected. Please see Lines 30.

L47: The results of Brandes et al. (2007) were limited to 52 cases over two winter seasons and isolated to a particular location. It doesn't seem correct to me to describe it as "climatological".

Reply: The "climatological" has been removed. Please see Lines 48.

L50-51: The meaning of "differentiation of riming degree" is unclear.

Reply: The sentence has been revised to improve the clarity. Please see Lines 51-52.

L54: Perhaps "above the 2DVD" would be clearer.

Reply: The sentence has been revised as per the reviewer's suggestion. Please see Line 55.

L55: I think that it is the difference that is minimized.

Reply: The sentence has been revised as per the reviewer's suggestion. Please see Line 55.

L61: I think "disdrometer" is more commonly used.

Reply: The “distrometer” has been revised to “disdrometer”. Please see Line 69.

L64: "transmits" instead of "transmitted".

Reply: The “transmitted” has been revised to “transmits”. Please see Line 71.

L65: "scatters" instead of "scattered".

Reply: The “scattered” has been revised to “scatters”. Please see Line 72.

L67: See earlier comment re "distrometer".

Reply: The “distrometer” has been revised to “disdrometer”. Please see Line 74.

L73-74: The meaning of "regarded as the self-evaluation of our result" is not clear.

Reply: The "regarded as the self-evaluation of our result" has been removed to improve the clarity. Please see Lines 81-82 in the revised manuscript. Or see the following.

Subsequently, the measurement of Z_{HH} weighted fall velocity (V_z) from MRR is compared with the calculated V_z from the derived bulk density and Parsivel PSD measurement.

Instruments and Data Processing *****

L85: Horizontal wind can cause problems with Pluvio and Parsivel measurements. Was any filtering or correction applied based on ambient wind speed?

Reply: All of the Pluvios were equipped with double windshields. The Pluvio at the MHS was within the DFIR (double fence intercomparison reference) in addition to the double shield. The environmental conditions of all sites are introduced in the revised manuscript, please see Lines 99-102 in the revised manuscript. Or see the following.

All of the Pluvios were equipped with double windshields. The Pluvio at the MHS was within the DFIR (double fence intercomparison reference) in addition to the double shield. All the sites investigated in this study have no taller trees or buildings near the MRR antenna and Parsivel. Each site's detailed layout and information can be found in Kim et al. (2021).

L90-91: What are the elevations of the sites?

Reply: The elevations of each site are, YPO (772 m MSL), MHS (789 m a.m.s.l.), CPO (855 m MSL), BKC (175 m MSL), and GWU (36 m MSL). Each site's detailed layout and

information can be found in Kim et al. (2021). The reference has been added to the revised manuscript. Please see Lines 96-98.

L93-95: Is it actually the PSD data that were filtered (PSD data do not include fall velocities)? Or was it the single-particle size and fallspeed data that were filtered? How does this filtering affect the calculated PSDs? Does it reduce particle counts?

Reply: The Parsivel single-particle size and fallspeed data were filtered. The minute Parsivel data was quality-controlled using the fall velocity filtering technique (Lee et al. 2015). The filtering removes the outlier particles, reducing particle counts. Subsequently, the PSD was calculated from the filtered data. The manuscript has been revised to improve clarity. Please see Lines 107-110 in the revised manuscript. Or see the following.

The minute Parsivel data was quality-controlled using the fall velocity filtering technique (Lee et al. 2015). The mean fall velocity and standard deviation (σ) for a given diameter were calculated, and the particles that deviate from the mean fall velocity of more than one standard deviation were filtered. The quality-controlled Parsivel data was subsequently processed to derive the PSD.

L96: What is the vertical resolution of the MRR data? What is the altitude above ground level of the third gate?

Reply: The MRRs had the same configuration during ICEP-POP; the vertical resolution was 150 m, and there were 31 gates up to 4.65 km. The third gate is 450 m above ground. The vertical resolution information has been added to the revised manuscript. Please see Lines 111-114 in the revised manuscript. Or see the following.

The MRRs had the same configuration during ICEP-POP; the vertical resolution was 150 m, and there were 31 gates up to 4.65 km. The MRR data was post-processed using the algorithm from Maahn and Kollias (2012). The sensitivity of MRR has been enhanced, and the Doppler velocity has been dealiased. The third gate (450 m above ground) of Z_{HH} data from MRR was selected to retrieve snow density since the first two gates contain some clutter contamination.

L104-106: "Bias" already implies that an average was taken, no need to say "mean bias". What are the standard deviations of the differences between the MRR Z_{HH} and the simulated Z_{HH} ? This would provide some insight into the uncertainty of the bias estimates.

Reply: The "mean bias" has been revised to "bias" per the reviewer's suggestion. The number concentration plot of MRR measured reflectivity, and Parsivel PSD calculated reflectivity, as shown below in Figure R2. The standard deviation of the differences

between them is about 1.1 to 1.3 dB for each site (shown in Table 2 of the revised manuscript). As the reviewer indicates, the standard deviation value can be considered the MRR reflectivity uncertainty. The standard deviation will be further applied to investigate the bulk density retrieval uncertainty.

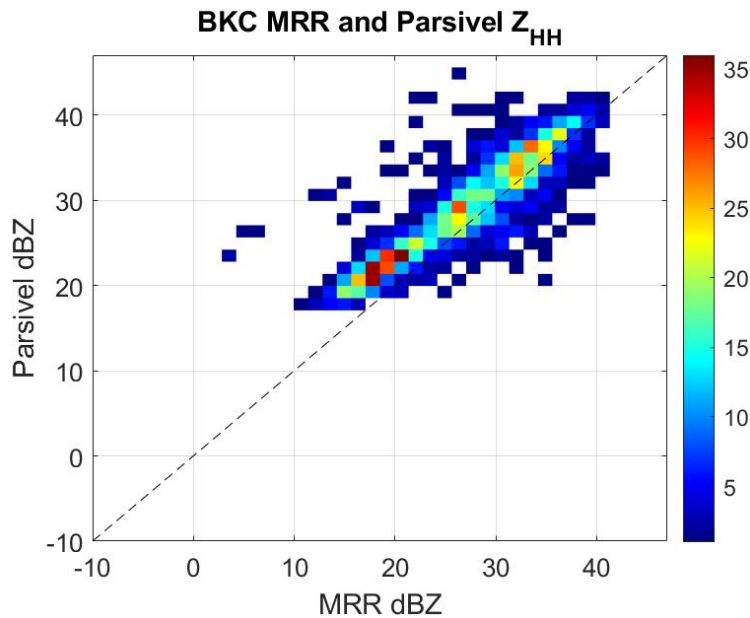


Figure R2: The number concentration distribution of measured reflectivity from MRR and simulated reflectivity from Parsivel of BKC site. The bias is -2.1 dBZ, and the standard deviation is 1.28 dBZ.

Methodology *****

L107: In the entirety of the Methodology section, there is no discussion of how uncertainties are determined for the retrieved properties or properties derived from the retrieval results.

Reply: As per the reviewer’s suggestion, the retrieval uncertainty has been investigated and summarized in the revised manuscript. With 1.2 dB MRR reflectivity uncertainty, the retrieval bulk density uncertainty is about 0.023 g cm⁻¹. A Discussion section has been added to the revised manuscript. **Please see Lines 358-417 in the revised manuscript. Or see the reply to "comment A" shown previously, pages 7-9.**

L112-114: It is unclear why the Huang et al. study is introduced at the beginning of the methodology. The Rayleigh assumption used by Huang et al. is clearly not appropriate for K-band radar (MRR) observing snowfall, so equation 2 is not applicable. The actual equation for estimating Z_{HH} using T-matrix backscatter cross-sections and attenuation is never presented or discussed.

Reply: Authors agree with the reviewer’s comment. Since T-matrix simulation is used and the Rayleigh assumption is not used in the retrieval algorithm, equation 2 has been revised. The reference has also been changed to Bringi and Chandrasekar (2001). The sentence of Rayleigh assumption is removed to improve the manuscript's clarity. Please see Lines 130-134 in the revised manuscript. Or see the following.

The sum of the values of v_i and v_w equals one or less than one if it contains air in the particle. Thus, the reflectivity factor (Z_{HH}) can be calculated as follows (Bringi and Chandrasekar 2001),

$$Z_{HH} = \left(\frac{\rho_{bulk}}{\rho_{ice}}\right)^2 \frac{|K_{ice}|^2 \lambda^4}{|K_w|^2 \pi^5} \int \sigma(D)N(D)dD; mm^6 m^{-3}. \quad (2)$$

The K_{ice} and K_w are the dielectric factors of solid ice and liquid water, respectively. σ is the backscattering cross-section, D is the particle size, and $N(D)$ is the particle size distribution. As shown in (1) and (2), the Z_{HH} is positively correlated to ρ_{bulk} .

L121: "modified from Huang et al.", I believe.

Reply: The typo has been corrected. Please see Line 138.

L126-127: More details are needed here. How were the dielectric properties of the mixed ice/liquid/air particles determined? How was the liquid water assumed to be distributed within a particle?

Reply: The ice and water are evenly distributed within the particle. The manuscript has been revised to improve the clarity. The sentence “The ice and water are assumed to be evenly distributed within the particle.” has been added, please see Lines 144-145.

L128-130: It’s not clear to me why spherical shapes were assumed just because the snow particles are observed from the bottom. I believe the particles would still appear to be non-spherical. It is not clear that spherical particle T-matrix calculations are appropriate for modeling snowflake backscattering a K-band.

Reply: Non-spherical and spherical particles do appear differently when looking upward. However, the orientation of the non-spherical particle is assumed to be isotropic and homogeneous. A sensitivity investigation assuming the particle axis ratio of 0.5 has been conducted. The results show that about 1.5 dBZ variation of simulated reflectivity can be induced due to the assumption of particle size.

A random error of MRR reflectivity with a standard deviation of 1.2 dB is introduced to imitate the particle assumption and MRR measurement uncertainty to the

retrieval uncertainty. The overall standard deviation of bulk density retrieval is about 0.025 (g cm^{-3}) for a given MRR reflectivity uncertainty of 1.2 dB. The bulk water fraction retrieval has the same feature, and the uncertainty is about 0.041. Please see the Discussion section in the revised manuscript, **Lines 358-417. Or see the reply to "comment A" shown previously, pages 7-9.**

L138-144: Something seems off about the results shown in Figure 2. The size distribution in panel (a) shows the size distribution consists of small particles and that the concentrations of those particles are small. I would expect the radar reflectivity to be small, in the neighborhood of 0 to 3 dBZ with typical ice densities for snowflakes based on other field experiment results I've examined with similar size distributions. Yet according to the dashed blue line in panel (b) the calculated reflectivity reaches over 18 dBZ, even with very small ice densities and virtually no liquid water.

Please check these calculations.

Reply: The calculated reflectivity values reaching over 18 dBZ are due to the high water fraction and dielectric constant. The calculated reflectivity from PSD ranges from -5 to 35 dBZ, and the values cover 0 to 3 dBZ (low ice and water fraction). The 18 dBZ is the reference reflectivity value from MRR to constrain the retrieved bulk density. We will use the bulk density retrieval from the precipitation imaging package (PIP) to verify the calculation of T-Matrix simulation and retrieved density.

The PIP, a video disdrometer, provides the PSD, fall speed, density, and snowfall rate of hydrometers (Newman et al., 2009; Pettersen et al., 2020) was also deployed at the MHS site during ICE-POP 2018. Tokay et al. (2023) have utilized PIP to investigate the PSD parameters, including mass-weighted diameter and normalized intercept. The bulk density is estimated by Tokay et al. (2023) with various assumptions. The PIP retrieved density was generated from the assumption that $D_{\max} = 1.15 D_{\text{eq}}$, and the mass derivation included was based on Bohm (1989). The time series of retrieved bulk density from the proposed algorithm and PIP are shown in Fig. R1.

We change the data time of Figure 2 to 1559 UTC in the revised manuscript. The PSD has a higher concentration of particles, thus the reflectivity values range from -5 to 50 dBZ. The MRR reference reflectivity is 22.23 dB. Please see the Fig. 2 in the revised manuscript. As shown in Fig. R1, the retrieved bulk density from the proposed algorithm (blue and red dots) and the PIP (gray dots) are in good agreement. The bulk density was about $0.07 (\text{g cm}^{-1})$ from both methods. The consistency of retrieved bulk density confirms the calculation of the bulk density and the simulated reflectivity from PSD. The discussion of the consistency between the proposed method and the PIP has been included in the

revised manuscript. **Please see Lines 398-413 (the Discussion, 5.3 section) in the revised manuscript. Or see the reply to "comment A" shown previously, pages 8-9.**

L145-150: I don't see this recommendation in Huang et al., so I think it is necessary to explain more fully the reasoning for this approach and to describe more completely the details of the approach. Do you mean that given the observed reflectivity, you would just pick the largest v_i that reproduces that reflectivity? Why?

Reply: One difference between our algorithm and Huang et al.'s (2010) is the assumption of the particle composition. Huang et al. (2010) assumed that a mixture of snow contains only ice and air. Please see page 642 of Huang et al. (2010), "To calculate the backscattering properties of the particles measured by the 2DVD, we consider snow to be a mixture of ice and air." The assumption of only ice and air from Huang et al. (2010) is the same as the v_w (water fraction) equals zero in Fig. 2b. The bottom part of Fig. 2b (e.g., $v_w = 0$) is exactly the same as Huang et al. (2010).

In our proposal algorithm, the reflectivity calculation fully considers water/ice/air fractions. Therefore, various water/ice/air fraction combinations can be derived from the matched reflectivity between MRR measurement and Parsivel calculation. The bulk density with maximum v_i (minimum v_w) with maximum bulk density is selected to determine the bulk snow density from these possible combinations of v_w/v_i . Assuming the minimum water fraction is similar to Huang et al. (2010)'s assumption. The manuscript has been revised to improve the clarity, **please see Lines 157-171. Or see the following.**

A selected example of the simulated Z_{HH} from observed PSD with various combinations of v_i/v_w is shown in Figure 2. The observed PSD from Parsivel (Fig. 2a) was applied to the T-Matrix backscattering simulation. All possible combinations of v_i/v_w were applied to calculate simulated Z_{HH} (Fig. 2b). The corresponding bulk density was derived via (1) and shown as contour dash lines in Fig. 2b. The values of simulated Z_{HH} vary from 0 to 50 dBZ (shaded color in Fig. 2b). The simulated Z_{HH} values increase with increasing of the bulk snow density. In this selected case, the observed Z_{HH} from MRR was 22.23 dBZ (dashed blue line in Fig. 2b). The observed Z_{HH} from MRR was thus applied to constrain the possible combination of v_i/v_w and bulk density. The possible ranges of v_i/v_w are 0.0/0.009 to 0.08/0.0, shown as a dashed blue line in Fig. 2b. The corresponding bulk densities are 0.009 and 0.074 (g cm^{-3}), respectively. The higher the fraction of ice (e.g., v_i), the higher bulk snow density values can be found in Fig. 2b. To determine the bulk snow density from possible combinations of v_i/v_w , the maximum bulk density with maximum v_i is selected. Choosing the bulk density with maximum v_i ensures the minimum value of v_w . This assumption is similar to Huang et al. (2010), which assumes that a mixture of snow contains only ice and air. The water fraction is not considered

in Huang et al. (2010). Therefore, the contour's maximum density in Fig. 2(b), 0.074 g cm^{-3} , is determined by assuming v_i and v_w are 0.08 and 0.0, respectively. Subsequently, the v_w is regarded as "bulk water fraction," which can also be estimated in the proposed method, in addition to the bulk density, and will be analyzed in the following section.

L149-153: This part of the methodology also requires more complete explanation and evidence. I'm not sure I follow and agree with your argument here.

Reply: The bulk water fraction is derived along with the maximum possible bulk density in the proposed method in this study. If a different assumption is made when selecting possible bulk density, the retrieved bulk water fraction will be different. Therefore, the performance of the retrieved bulk water fraction is linked with bulk density retrieval. Since there are no direct measurements of bulk water fraction, we will compare the retrieved bulk density from the proposed method and PIP. The consistency between retrieved bulk density from the two algorithms confirms that the retrieved bulk water should be reasonable.

As shown in Fig. R1(a), the retrieved bulk density values from the proposed algorithm and PIP gradually decrease from nearly 1.0 to $0.1 \text{ (g cm}^{-3}\text{)}$ between 03 and 06 UTC. Both algorithms capture the transition from the mixing-phase to dry snow. Please see Figure R1. The manuscript has been revised to include the discussion of the bulk water fraction retrieval. **Please see Lines 398-413 (the Discussion, 5.3 section) in the revised manuscript. Or see the reply to "comment A" shown previously, pages 8-9.**

Since T-matrix is being used rather than equation (2), it may not be clear to many readers how the liquid and ice water dielectric factors come into play. I expect you are using some form of mixing rule (e.g., Maxwell-Garnet?). I think explanation needs to be provided about how the particle dielectric properties are determined for a mixture of ice and liquid water and how this influences backscattering properties as v_i and v_w change.

Further, Figure 2b seems to show that there is only a narrow range of the solution space ($v_w = 0.015$ to 0.1 with $v_i < 0.5$) for which Z might be said to be moderately more sensitive to v_w than to v_i due to liquid water's larger dielectric constant. Also, how is this sensitivity to v_w influenced by your method for choosing v_i ? Clearly, if you pick the maximum v_i for this case, there is much weaker sensitivity of Z to v_w . Finally, it is not clear what is meant by "The change of v_w can be ... obtained ...".

Reply: In reply to the previous comment, the performance of the retrieved bulk water fraction is linked with bulk density retrieval. Since there are no direct measurements of bulk water fraction, we will compare the retrieved bulk density from the proposed

method and PIP. The retrieved bulk density values from the proposed algorithm and PIP gradually decrease from nearly 1.0 to 0.1 (g cm⁻³) between 03 and 06 UTC in Fig R1(a). Both algorithms capture the transition from the mixing-phase to dry snow. Please see Figure R1. The manuscript has been revised to include the discussion of the bulk water fraction retrieval. **Please see Lines 398-413 (the Discussion, 5.3 section) in the revised manuscript. Or see the reply to "comment A" shown previously, pages 8-9.**

The mixing rule of Maxwell-Garnet is applied to the T-Matrix calculation. The influence of vi/vw composition on the backscattering properties has been discussed in the manuscript. **Please see Lines 133-135 in the revised manuscript. Or see the following.**

The K_{ice} and K_w are the dielectric factors of solid ice and liquid water, respectively. σ is the backscattering cross-section, D is the particle size, and $N(D)$ is the particle size distribution. As shown in (1) and (2), the Z_{HH} is positively correlated to ρ_{bulk} . The higher hydrometer bulk density has a higher value of Z_{HH} for a given PSD.

L153-156: For clarity, I would briefly describe both approaches here, then follow with more detailed descriptions of each one. What is meant by "self-verified"?

Reply: The description has been revised to improve the clarity. The original purpose of utilizing reflectivity-weighted velocity to filter adequate retrieval is no longer needed and has been removed in the revised manuscript. The quality retrieval results have been greatly improved by applying the post-processed MRR data per the reviewer's suggestion. The low SNR MRR measurement has been removed. The comparison of reflectivity-weighted velocity is mainly used to identify the inadequate retrieval due to the attenuation effect on MRR reflectivity. Please see Lines 185-187 in the revised manuscript. Or see the following.

The comparison of V_Z^{MRR} and $V_Z^{\rho_{bulk}}$ is considered an overall validation of the retrieved bulk density. In addition, the inconsistency between the $V_Z^{\rho_{bulk}}$ and the V_Z^{MRR} can identify inadequate bulk density retrieval. For example, the attenuation effect can lead to underestimating the MRR reflectivity measurement and, thus, underestimating the retrieved bulk density.

L157-165: This is for spherical particles. Do you assert it is appropriate for snow particles? How does this relationship compare with Mitchell and Heymsfield (2005) or Heymsfield and Westbrook (2010)? These newer fallspeed models are more appropriate for snowflakes.

Reply: Per the reviewer's suggestion, the retrieval results have significantly improved after applying the post-processed MRR data (Maahn and Kollias 2012). The noisy bulk

density has been removed. The original purpose of removing inadequate bulk density retrieval by reflectivity-weighted velocity is no longer needed. The reflectivity-weighted velocity comparison is obtained for two purposes. First, the comparison intends to examine the overall performance of the retrieved bulk density. The overall consistency is shown in Fig. 3. Second, the “bulk density-derived” reflectivity-weighted velocity is obtained to identify antenna attenuation issues as shown in Fig. 5(e). The issue of spherical particle assumption on terminal velocity calculation has been discussed in the revised manuscript. **Please see Lines 218-221 in the revised manuscript. Or see the following.**

The various shapes aerodynamically complicate the falling behaviors of ice-phase and mixed-phase particles (Mitchell and Heymsfield 2005; Heymsfield and Westbrook 2010). Moreover, various measurement issues of MRR and Parsivel also induce some inconsistency. Nevertheless, the overall consistency of the V_Z^{MRR} and V_Z^{Pbulk} suggests that the retrieved bulk density is an adequately reasonable value.

L166-167: This is not a correct statement. Both V_Z _MRR and Z _MRR (which is used to constrain the retrieval) are derived from the same basic measurements of Doppler spectra. So they are not independent.

Reply: The manuscript has been revised as per the reviewer’s suggestion. Please see Lines 185-187.

L168-169: But what were this "various issues"?

Reply: The manuscript has been revised as per the reviewer’s suggestion. Please see Lines 185-187.

L170-171: So, my understanding is that, for the data presented in the results, any retrievals with retrieved V_Z greater than observed V_Z plus one standard deviation are excluded. Is that correct? How does the 1-sigma uncertainty in the observed V_Z compare against the 1-sigma uncertainty in the retrieved V_Z ?

Reply: The V_Z criteria for removing inadequate bulk density retrieval is no longer needed. As per the reviewer’s suggestion, the retrieval results have significantly improved after applying the post-processed MRR data (Maahn and Kollias 2012). The noisy bulk density has been removed. The V_Z difference is mainly used to identify the attenuation effect of MRR reflectivity. **Please see Lines 185-187. Or the reply to “L153-156” on page 10.**

L176: I think the term on the right of the summation needs to be multiplied by the size bin width (ΔD_i) before summation.

Reply: The typo has been corrected. Please see Line 191.

L178: Perhaps "compared against" rather than "examined with".

Reply: The sentence has been revised as per the reviewer's suggestion. Please see Line 193.

Results *****

L184: The Results contain no assessments of uncertainties in the observations (Z_{HH} , V_z , PSD, SR), in the retrieved properties (bulk particle density, bulk liquid water fraction), or in the properties derived from the retrieval results (Z_{HH} , V_z , SR). How are we to determine if the retrieval results and V_z and SR biases, for example, are significant or not?

Reply: As per the reviewer's suggestion, the discussion of the retrieval uncertainty has been included in the revised manuscript. Please see the Discussion section for more details. (Lines 358-417). Or see the reply to "comment A" shown previously, pages 7-9.

Reflectivity-weighted (V_z) =====

L197: -0.27 to 0.03 is the range in bias values only, not related to standard deviation.

Reply: The V_z has been recalculated by using post-processed MRR data. The values of standard deviation are provided in the submitted manuscript. The sentence has been revised to improve the clarity. Please see Lines 206-216 in the revised manuscript. Or see the following.

4.1 Reflectivity-weighted (V_z)

The normalized number density function of measured V_z^{MRR} from MRR and "density-calculated" $V_z^{\rho_{bulk}}$ from Parsivel PSD of five sites are shown in Fig. 3. The V_z^{MRR} and $V_z^{\rho_{bulk}}$ are in agreement with each other. The majority of the data show reasonably consistent values. The GWU site had the most consistent velocity. On the other hand, YPO, MHS, and CPO sites had second peak values of about 2.0-3.0 $m\ s^{-1}$ of V_z^{MRR} and 1.0-2.0 $m\ s^{-1}$ of $V_z^{\rho_{bulk}}$. In general, the $V_z^{\rho_{bulk}}$ values of YPO, MHS, CPO, and are slightly lower than V_z^{MRR} . The bias values (Table 3) are about -0.81 ms^{-1} to 0.01 ms^{-1} . The standard deviation values are about 1.02 to 1.88 ms^{-1} , respectively. All sites combined mean bias and standard deviation values are -0.46 ms^{-1} and 1.35 ms^{-1} , respectively. It is postulated that the lower values of $V_z^{\rho_{bulk}}$ than of V_z^{MRR} is

caused by the attenuation effect on the MRR reflectivity. The attenuated reflectivity leads to underestimation of retrieved bulk density and "density-calculated" $V_z^{P_{bulk}}$. An example of attenuated reflectivity will be discussed in the case study of 28 February 2018. The retrieved bulk density influenced by the attenuation effect will be identified and removed by visual examination of V_z comparison.

L199: Clarify that this is the bias and standard deviation for all site results combined.

Reply: The bias and standard deviation are all site results combined. The sentence has been revised to improve the clarity. Please see Lines 212-213 in the revised manuscript.

L200-201: It would be appropriate to acknowledge this limitation earlier in the paper where the method is introduced.

Reply: More discussion has been added to the revised manuscript. Please see Lines 217-221.

L203: Usually, "mixed-phase".

Reply: The typo has been corrected. Please see Line 219.

L203-204: Again, there is a vague reference to "measurement issues", but there has been no descriptive discussion or quantification of them.

Reply: The discussion has been revised. Please see Lines 214-221.

L206-207: This kind of filtering (omitting data from further analysis simply because the data don't give results that match other observations) tends to negate or reduce the believability of the proposed method. This is especially true when the authors cannot point to specific physical conditions that caused the method to fail. How much data was filtered at this stage? How poor are the subsequent results if the data are not filtered?

Reply: The V_z criteria for removing inadequate bulk density retrieval is no longer needed. Per the reviewer's suggestion, the retrieval results have significantly improved after applying the post-processed MRR data (Maahn and Kollias 2012). The noisy bulk density due to low SNR has been removed. The post-processed MRR data has greatly improved its sensitivity. The V_z difference is mainly used to identify the attenuation effect of MRR reflectivity. Please see Lines 215-216 of the revised manuscript. Or see the following.

The retrieved bulk density influenced by the attenuation effect will be identified and removed by visual examination of V_z comparison.

Liquid-equivalent snowfall rate (SR) =====

L215-216: Snow gauges like the Pluvio can have problems with undercatch when surface winds are strong. Were the winds checked and any filtering or corrections applied? The bias in the density-derived SR versus the Pluvio SR might be worse if the Pluvio data are corrected for undercatch.

Reply: All of the Pluvios were equipped with double windshields. The Pluvio at the MHS was within the DFIR (double fence intercomparison reference) in addition to the double shield. The environmental conditions of all sites are introduced in the revised manuscript, please see Lines 99-102. Or see the following.

All of the Pluvios were equipped with double windshields. The Pluvio at the MHS was within the DFIR (double fence intercomparison reference) in addition to the double shield. All the sites investigated in this study have no taller trees or buildings near the MRR antenna and Parsivel. Each site's detailed layout and information can be found in Kim et al. (2021).

L216-219: This is the first mention of snow/ice accumulation on the MRR antenna. It would be appropriate to mention that this occurred during the description of the observations earlier in the paper.

Reply: The revised manuscript has added a discussion of the attenuation effect of MRR due to snow/ice accumulation on the antenna. Please see Lines 213-216 in the revised manuscript. Or see the following.

It is postulated that the lower values of $V_Z^{P_{bulk}}$ than of V_Z^{MRR} is caused by the attenuation effect on the MRR reflectivity. The attenuated reflectivity leads to underestimation of retrieved bulk density and "density-calculated" $V_Z^{P_{bulk}}$. An example of attenuated reflectivity will be discussed in the case study of 28 February 2018. The retrieved bulk density influenced by the attenuation effect will be identified and removed by visual examination of Vz comparison.

L224: Should be "moist air".

Reply: The typo has been corrected. Please see Line 238.

L227-228: For the case study of the 28 February event, why is only the MHS site data analyzed?

Reply: The 28 February 2018 event is selected to demonstrate the retrieval results. The consistency of SR calculated from retrieved bulk density and measurement from Pluvio indicate that the proposed algorithm performs reasonably well. The pronounced attenuation effect of MRR reflectivity and its impact on underestimating Vz are shown

to demonstrate the retrieval uncertainty. The other sites show almost the same evolution of the retrieved properties. In addition, the PIP was deployed at MHS and collocated with MRR and Parsivel. The comparison of retrieved bulk density from our method and PIP is discussed in the revised manuscript. Only the MHS site of 28 February is shown to keep the manuscript concise. A more detailed analysis of each site of 7 March 2018 is discussed.

Case study: 28 February 2018 =====

L258: Regarding "fall velocity was more significant than 1 m s^{-1} ", I suggest rewording this to avoid confusion with statistical significance.

Reply: The sentence has been revised to improve the clarity. Please see Line 271.

L263: Regarding "derivation density", do you mean "derived density"?

Reply: The typo has been corrected. Please see Lines 276.

L263-264: Are you describing the *maximum* particle sizes?

Reply: The typo has been corrected. Please see Lines 276.

Case study: 7 March 2018 =====

L268-269: "produced prominent precipitation" and "produced intensive precipitation" sounds like repetition, are both needed?

Reply: The "produced prominent precipitation" has been removed. Please see Lines 280-281.

L273-310: There are a number of locations on these lines that describe bulk water fraction. See my major comments above - I don't think the capability of the retrieval to distinguish and quantify bulk water fraction (or volume fraction of liquid water) has been demonstrated.

Reply: The bulk water fraction is derived along with the maximum possible bulk density in the proposed method in this study. If a different assumption is made when selecting possible bulk density, the retrieved bulk water fraction will be different. Therefore, the performance of the retrieved bulk water fraction is linked with bulk density retrieval. Since there are no direct measurements of bulk water fraction, we will compare the retrieved bulk density from the proposed method and PIP. The consistency between retrieved bulk density from the two algorithms confirms that the retrieved bulk water should be reasonable. Please see Figure R1.

As shown in Fig. R1(a), the retrieved bulk density values from the proposed algorithm and PIP gradually decrease from nearly 1.0 to 0.1 (g cm⁻³) between 03 and 06 UTC. Both algorithms capture the transition from the mixing-phase to dry snow. Please see Figure R1 in the previous reply. The manuscript has been revised to include the discussion of the bulk water fraction retrieval. **Please see Lines 398-417 in the revised manuscript. Or see the reply to "comment A" shown previously, pages 7-9.**

L286: Regarding "which are in accord with the distributions of all velocity-diameter relations", it is not clear to me what this means.

Reply: The sentence has been revised to "Overall, the retrieved bulk density and bulk water fraction successfully reveal distinct fall velocity-diameter relations of each site due to the different synoptic environments." to improve clarity. Please see Lines 295-296.

L288: Regarding "They gradually dissipated", it is not clear what "They" is referring to.

Reply: "They" refers "the precipitation". The sentence has been revised to improve the clarity. Please see Lines 299.

L293-294: Regarding "Hence, it implies more ... confirm the distribution of fall velocity and diameter". The meaning here is not clear to me.

Reply: The sentence has been revised to "The high bulk density (about 0.9 g cm⁻³) period corresponds to a higher bulk water fraction from 0.4 to 0.8." to improve clarity. Please see Lines 302-303.

L296: Regarding "confirmed by the alike contrast", the meaning of "alike contrast" is not clear.

Reply: The sentence has been revised to "The higher density initially in MHS and BKC sites are also confirmed by the same contrast between 08 to 19 UTC on 7 March (Figs. 12a, b) than 19 UTC to 03 UTC on 8 March (Figs. 12d, e)." to improve the clarity. Please see Lines 306-308.

L298: Not true, YPO, MHS and CPO, BKC show mostly near-zero bulk water fraction. For most of this discussion, need to be clear about when only-elevated, only-coastal, or all sites are being described.

Reply: Only BKC and GWU feature high bulk water fractions. The sentence has been revised to improve the clarity. The sentence has been revised to "the BKC and GWU sites featured high bulk density and bulk water fraction (Figs. 10a-11a)." to improve clarity. Please see Line 309.

L300: "Transited" should be "transitioned".

Reply: The type has been corrected. Please see Line 312.

Statistical analysis of bulk density and bulk water fraction

L317-320: What is the basis of the assertion that Brandes et al. (2007) observations were dominated by "almost spherical aggregates"? Brandes et al. appear to have used the equivalent volume diameter as determined by the 2DVD software, as particle sizes. These, will be different than the particle size determined by the Parsivel. Brandes et al. do use the median volume diameter to parameterize the bulk density; however it is not evident that the cases in this study and those of Brandes et al. involved similar meteorological conditions. Evidence should be presented for this claim.

Reply: The statement “dominated by almost spherical aggregates” can be found in the abstract of Brandes et al. (2007). Considering distinct environmental conditions, instrumentations, and retrieval techniques, most of the particles in this study are consistent with the $\rho_{bulk} - D_m$ relation from Heymsfield et al. (2004) and $\rho_{bulk} - D_0$ from Brandes et al. (2007). These results indicate that the proposed bulk density estimation algorithm can derive reasonable retrievals with statistically consistent microphysical characteristics from previous studies. The manuscript has been revised to improve the clarity. Please see Lines 324-338 in the revised manuscript. Or see the following.

The retrieved bulk density and bulk water fraction are investigated statistically to understand the microphysical characteristics of the winter precipitation systems from ICE-POP 2018 and its pre-campaign. Fig. 13 shows the number concentration of retrieved bulk density and observed mass-weighted diameter (D_m) from PSD of all sites. The bulk density decreases exponentially as D_m increases. Heymsfield et al. (2004) utilized the aircraft data collected from two field programs, namely the Atmospheric Radiation Measurement (ARM) program, Cirrus Regional Study of Tropical Anvils and Cirrus Layers (CRYSTAL) Florida Area Cirrus Experiment (FACE) in southern Florida during July 2002. The ARM data is mostly ice clouds formed primarily through large-scale ascent, and the CRYSTAL observations are mainly from convectively generated cirrus anvils. Brandes et al. (2007) utilized the data of 52 storm days from the Front Range in eastern Colorado during October–April 2003 to 2005 of a ground-based 2DVD. The data of Brandes et al. (2007) is dominated by almost spherical aggregates having near-exponential or superexponential size distributions. The $\rho_{bulk} - D_0$ relation (D_0 , median volume diameter) from Brandes et al. (2007) is replaced by D_m in Fig. 13 for

comparison, assuming the exponential PSD and $D_m = 4D_0/3.67$.

Despite distinct environmental conditions, instrumentations, and retrieval techniques, most of the particles in this study are consistent with the $\rho_{bulk} - D_m$ relation from Heymsfield et al. (2004) and Brandes et al. (2007). These results indicate that the proposed bulk density estimation algorithm can derive reasonable retrievals with statistically consistent microphysical characteristics from previous studies.

L321-325: The particle sizes used in Heymsfield et al. (2004) are derived from aircraft particle probes, as you have noted. These particle sizes are probably more like the "maximum dimension" of the particle and less like the "equivalent diameter" determined by a Parsivel. Additionally, Heymsfield et al. relate density to mass mean diameter, not to median volume diameter. So the comparison described here is somewhat an "apples to oranges" comparison. It is not surprising there are differences.

Reply: Since the two papers use different parameters (D_m and D_0) to present mean size, we convert D_0 to D_m by assuming exponential PSD ($D_m = 4D_0/3.67$). Moreover, the bulk density comparison among this study, Heymsfield et al. (2004), and Brandes et al. (2007) does not intend to emphasize the difference. The discussion has been rephrased. The Figure has been revised. **Please see Figure 13 and Lines 324-338. Or see the reply to previous comments.**

L335-344: As I noted above, I am not convince that this method is capable of accurately distinguishing and quantifying the liquid and ice volume ratios and the corresponding bulk water fraction. Also, although it is asserted that there are differences in the meteorology of the warm-low and cold-low events (i.e., "warmer and moister environments" for the warm-low events), no meteorological data is provided to support this.

Reply: As per the previous comments and replies, we have compared the retrieved bulk density from the proposed algorithm and PIP retrieval (see below figures) and the SR with Pluvios. The bulk water fraction is derived along with the maximum possible bulk density in the proposed method in this study. If a different assumption is made when selecting possible bulk density, the retrieved bulk water fraction and density will be different. Therefore, the performance of the retrieved bulk water fraction is linked with bulk density retrieval. Since there are no direct measurements of bulk water fraction, we compared the retrieved bulk density from the proposed method and PIP. The consistency between retrieved bulk density from the two algorithms confirms that the retrieved bulk water should be reasonable.

As shown in Fig. R1(a), the retrieved bulk density values from the proposed

algorithm and PIP gradually decrease from nearly 1.0 to 0.1 (g cm^{-3}) between 03 and 06 UTC. Both algorithms capture the transition from the mixing-phase to dry snow. Please see Figure R1 in the previous reply. The manuscript has been revised to include the discussion of the bulk water fraction retrieval. **Please see Line 398-417. Or see the reply to "comment A" shown previously, pages 8-9.**

In reply to the previous comment, the temperature ($^{\circ}\text{C}$) and water vapor pressure (hPa) measurements from nearby mountain and coastal AWS sites are collected and summarized in Fig. 14e. The warm-low events have warmer and moister conditions compared to cold-low events. The coastal area's warm- and cold-low events have similar mean temperature values. On the other hand, the water vapor pressure increases significantly from cold-low to warm-low events. The mountain area has similar features but with higher temperature increments and fewer increments of water vapor pressure. **Please see Lines 351-357 in the revised manuscript. Or see the following.**

The temperature ($^{\circ}\text{C}$) and water vapor pressure (hPa) measurements from nearby mountain and coastal AWS sites are collected and summarized in Fig. 14e. Warm-low events have warmer and moister conditions than cold-low events. The coastal area's warm- and cold-low events have similar mean temperature values. On the other hand, the water vapor pressure increases significantly from cold-low to warm-low events in the coastal region. The mountain area has similar features, but higher temperature increments and fewer increments of water vapor pressure. These results indicate that the winter precipitation systems of coastal sites with warmer and moister environments have higher bulk density and bulk water fraction than mountain sites.

L345: It is probably more appropriate to say that the density of snow varies with "imposed weather conditions".

Reply: The sentence has been revised to improve the clarity. Please see Lines 419.

Conclusions *****

L347-350: As I've noted, I have concerns about the bulk water fraction estimates. I don't believe sufficient proof of the capability has been provided, and in no way has evidence been provided that the values are "precise". The high sensitivity of Z_{HH} to the liquid portion of the particle led to precise bulk water fraction estimation. It implied better capability of the density variation due to bulk water fraction change (ex. melting) in the proposed method in this study.

Reply: Thanks reviewer's suggestion. As per the previous comments and replies, we have compared the retrieved bulk density from the proposed algorithm and PIP retrieval (see

below figures) and the SR with Pluvios. The bulk water fraction is derived along with the maximum possible bulk density in the proposed method in this study. If a different assumption is made when selecting possible bulk density, the retrieved bulk water fraction will be different. Therefore, the performance of the retrieved bulk water fraction is linked with bulk density retrieval. Since there are no direct measurements of bulk water fraction, we compared the retrieved bulk density from the proposed method and PIP. The consistency between retrieved bulk density from the two algorithms confirms that the retrieved bulk water should be reasonable.

As shown in Fig. R1(a), the retrieved bulk density values from the proposed algorithm and PIP gradually decrease from nearly 1.0 to 0.1 (g cm⁻³) between 03 and 06 UTC. Both algorithms capture the transition from the mixing-phase to dry snow. Please see Figure R1 in the previous reply. The manuscript has been revised to include the discussion of the bulk water fraction retrieval. **Please see Line 398-417. Or see the reply to "comment A" shown previously, pages 8-9.**

L352: Clarify what is meant by "self-evaluation".

Reply: The sentence has been revised to "The reflectivity-weighted fall velocity (V_z) of MRR is applied to evaluate the retrieved bulk density and water fraction.". Please see Line 424 in the revised manuscript.

L357: There's no evidence shown that applying the V_z criteria improves the consistency of retrieved SR with observed SR.

Reply: The V_z criteria are no longer needed. Please see the revised manuscript, **Lines 424-427. Or see the following.**

The reflectivity-weighted fall velocity (V_z) of MRR is applied to evaluate the retrieved bulk density and water fraction. Inconsistency of measured V_z from MRR and calculated V_z from retrieved bulk density from 09 to 15 UTC on 28 February 2018 is noticed. It is postulated that the attenuation effect mainly causes the V_z discrepancy due to the accumulated snow on the MRR antenna.

L359: Is "all available cases" true? SR comparison are shown only for two cases at the sites.

Reply: The SR comparisons from the cases listed in Table 1 are summarized in Table 3. **Please see the revised manuscript, Lines 428-430. Or see the following.**

General consistency between the measured and the bulk density-calculated SR was found in

all available cases (Table 1) of the four sites during the ICE-POP 2018 campaign, as summarized in Table 3.

L364-365: I don't think this statement is supported. This study has investigated two cases which have similar synoptic setups and has found similarity of microphysical characteristics. But you haven't demonstrated that different synoptic setups will produce microphysical characteristics dissimilar to these.

Reply: The statement has been revised to avoid confusion and improve clarity. "The bulk density and bulk water fraction of two events with warm low synoptic patterns (28 February and 7 March 2018) were investigated." Please see Lines 431-435.

L366: I would suggest "contrasting" or "dissimilar" rather than "contrastive".

Reply: The typo has been corrected. Please see Line 436.

Tables and Figures *****

Table 3: Note previous comment about "mean bias". Also, why is the Vz criterion for "ALL" shown as "nan"? To help us understand the significance of the biases and standard deviations, please also include the associated mean values and standard deviations of the observed quantities.

Reply: The "mean bias" has been revised to "bias". The Vz criterion is no longer needed. The mean values of Vz and SR are provided. Please see Table 3 in the revised manuscript.

Figure 6: Is the colorbar axis labeled correctly? Were there really counts ranging up to $10^{*}50$?

Reply: The typo has been corrected. It should be $10^{*}5$. Please see Fig. 6 in the revised manuscript. Fig. 12 also has the same mistake and has also been corrected.

Figure 12: Why does the mountainous MHS site maintain a population of high-fall-velocity small particles throughout the 7-8 March event?

Reply: As indicated by the study from Battaglia et al. (2010), Parsivel's fall velocity measurement may not be accurate for a snowflake particle. This is due to the internally assumed relationship between horizontal and vertical snow particle dimensions. Friedrich et al. (2016) indicate that Parsivel can suffer from splashing of particles (observed as a small diameter with large fall velocity when particles fall on the head of the sensor) and margin fallers (observed as a faster velocity than true fall velocity when particles fall through the edge of the sampling area). Yuter et al. (2006), Aikins et al.

(2016), and Kim et al. (2021) indicate the splashing and border effects of the diameter of < 1 mm in Parsivel fall velocity measurements. The Parsivel data shown in Figure 12 was quality-controlled, as suggested by Lee et al. (2015). The discussion of fall velocity measurement uncertainty is added in the revised manuscript. **Please see Lines 105-109. Or see the following.**

Friedrich et al. (2016) indicate that Parsivel can suffer from splashing of particles (observed as a small diameter with large fall velocity when particles fall on the head of the sensor) and margin fallers (observed as a faster velocity than true fall velocity when particles fall through the edge of the sampling area). The minute Parsivel data was quality-controlled using the fall velocity filtering technique (Lee et al. 2015). The mean fall velocity and standard deviation (σ) for a given diameter were calculated, and the particles that deviate from the mean fall velocity of more than one standard deviation were filtered.